ACS ES&T Engineering

pubs.acs.org/estengg

Review

Wetting, Scaling, and Fouling in Membrane Distillation: State-of-the-Art Insights on Fundamental Mechanisms and Mitigation Strategies

Thomas Horseman, Yiming Yin, Kofi SS Christie, Zhangxin Wang, Tiezheng Tong,* and Shihong Lin*

Cite This: *ACS EST Engg.* 2021, 1, 117−140

Read Online

ACCESS | Metrics & More | Article Recommendations

ABSTRACT: Membrane distillation (MD) has been garnering increasing attention in research and development, since it has been proposed as a promising technology for desalinating hypersaline brine from various industries using low-grade thermal energy. However, depending on the application context, MD faces several important technical challenges that would lead to compromised performance or even process failure. These challenges include pore wetting, mineral scaling, and membrane fouling. This review is devoted to providing a state-of-the-art understanding of fundamental mechanisms and mitigation strategies regarding these three challenges. Guided by the fundamental understanding of each membrane failure mechanism, we discuss both operational and material strategies that can potentially address the three technical challenges. In particular, the material strategies involve the development of MD membranes with tailored special wetting properties to impart resistance against different types of membrane failure. Lastly, we also discuss research needs and best practices in future studies to further enhance our ability to overcome technical challenges toward the practical, sustainable, and scalable applications of MD.

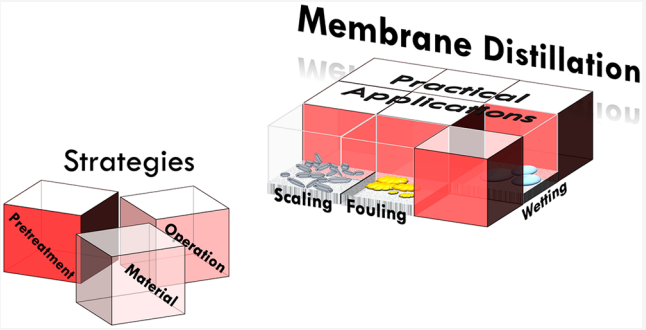

KEYWORDS: *membrane distillation, wetting, scaling, fouling, mitigation strategies*

INTRODUCTION

Membrane distillation (MD) is a membrane-based thermal desalination process that has received extensive and growing research and development interests in the past few decades. While MD has multiple configurations, each case involves the use of a nonwetted (typically hydrophobic), microporous membrane to serve as an airgap that separates the feed and distillate solutions from mixing. The transport of water vapor from the hot, salty feed solution to the cold distillate is driven by a partial vapor pressure gradient. This partial pressure gradient is typically induced by the temperature gradient and, in certain cases, enhanced by a partial vacuum.[1−3]

The interest in MD has grown substantially in recent years due to the increasing demand for modular systems capable of treating hypersaline water including oil- and gas-produced water, brine from inland brackish water desalination, and brine generated in zero liquid discharge (ZLD) processes.[4−7] Because of growing water scarcity and more stringent regulations, these hypersaline brines are becoming both unconventional sources of water and hazardous wastes of increasing environmental concern. MD is the most promising modular (down-scalable) technology capable of treating high-salinity feedwater using low-grade thermal energy and, thus, has several unique advantages for treating hypersaline brine, as compared to the state-the-of-art desalination process, reverse osmosis,[1,8,9] or conventional thermal distillation processes.[1,10−13] More recently, MD has also been explored as an advanced technological platform for solar-thermal desalination due to its ability to implement latent heat recovery.[14−16]

Another major category of membrane processes that envelopes MD is membrane contactor (MC), where a nonwetted microporous membrane is also used as an airgap. However, the intended species of mass transfer in MC is the volatile solute instead of water vapor. For instance, MC has been actively explored for recovering valuable gases such as ammonia and methane, sequestrating carbon dioxide, oxygenation/deoxygenation, and removal of volatile contaminants.[17,18] The mass transfer in an MC is also driven by a partial vapor pressure gradient, which is often induced by a concentration gradient and sometimes assisted by a thermal

Received: June 12, 2020
Revised: August 7, 2020
Accepted: August 11, 2020
Published: October 1, 2020

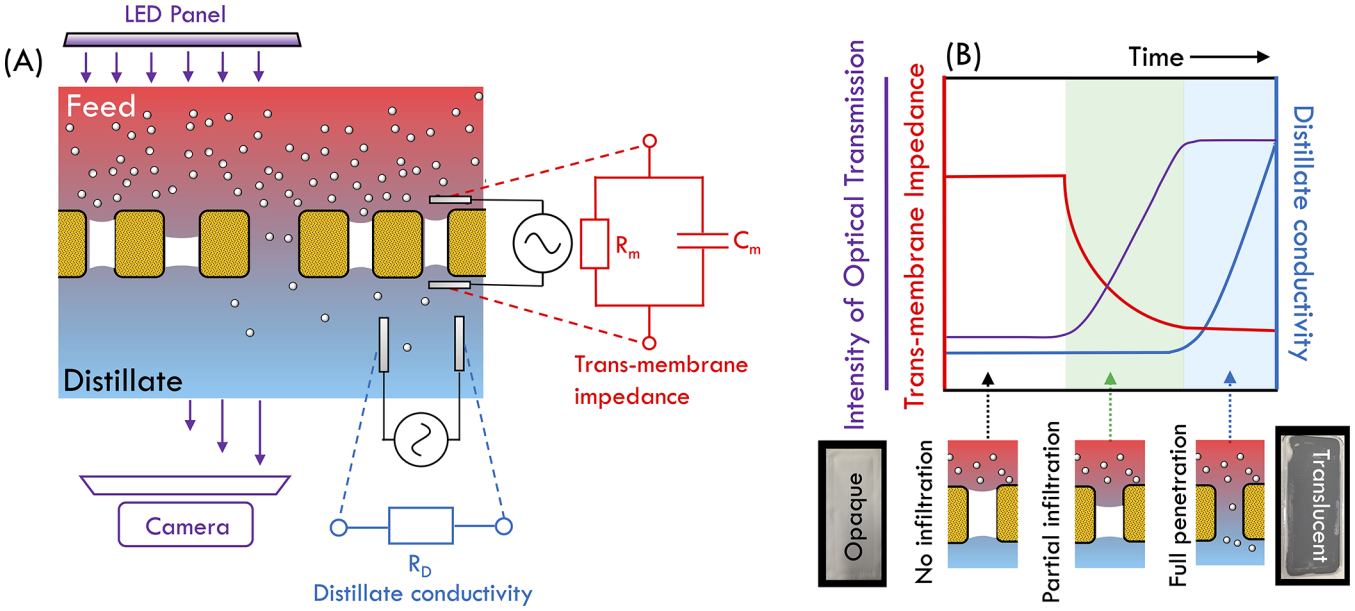

Figure 1. (A) Schematic diagram of membrane wetting, featuring three wetting detection techniques based on distillate conductivity, optical transmittance, and transmembrane impedance. (B) Illustration of how different properties associated with different detection techniques vary in different stages of the wetting process. We note that distillate conductivity only starts to increase when at least some pores are fully penetrated by the feed solution. Thus, the distillate conductivity does not capture any information when some pores are only partially infiltrated (but not a single pore has been fully penetrated). Detection techniques based on transmembrane impedance and optical transmittance can provide information regarding this stage of partial infiltration.

gradient and/or partial vacuum (fundamentally, all mass-transfer processes in MD and MC are driven by a chemical potential gradient reflected as a partial vapor pressure gradient).

In both MD and MC, the microporous membranes serve as not only a medium for vapor transport but also a barrier to direct liquid permeation and, thus, must be maintained free from pore blocking and wetting. However, the feedwater in many promising applications of MD or MC often contains constituents that promote fouling and wetting of conventional hydrophobic membranes.[19−24] For example, organic matter, such as proteins from the food and beverage industry or oil particles that exist in oil- and gas-produced water, are potent foulants, especially for hydrophobic membranes.[4,25−27] Low-surface-tension, water-miscible liquids may exist in the feedwater of MC, reducing the overall surface tension of the feedwater and resulting in pore wetting.[28,29] In addition, synthetic surfactants and natural amphiphiles may also reduce the surface tension of the feedwater and induce wetting.[30−32] For MD used in treating hypersaline brine, an additional challenge is mineral scaling, that is, the formation and/or accumulation of salt precipitates on the membrane surface that results in significant flux reduction and, in some cases, even pore wetting.[33−35]

All these technical challenges, namely, wetting, scaling, and fouling, constrain the practical adoption of MD and MC for treating a wide spectrum of feedwater. In particular, these limitations pose a paradox for MD as an effective technology for desalinating and concentrating hypersaline brines: on the one hand, MD is very promising for such applications due to its (theoretical) capability of handling hypersaline brine using low-grade thermal energy; on the other hand, concentrating brine inevitably increases the concentrations of salts, foulants, and surfactants—whatever constituents that originally exist in the feedwater—and thus intensifies the propensity of scaling, fouling, and wetting and limits the (practical) applicability of MD in various applications.[1,9,36−38] It is therefore of paramount importance for the community to gain fundamental understanding of these challenges facing MD and MC and to develop effective strategies of mitigating these technical challenges to enable these membrane-based vapor-transport processes to achieve their full potential for practical applications. This review is precisely organized to assess the recent advances in the fundamental understanding and technological development we have made as a community toward addressing these technical challenges.

In this review, we will discuss the fundamental mechanisms and mitigation strategies for the three technical challenges in membrane-based vapor-transfer processes: wetting, mineral scaling, and fouling. We will focus our discussion on MD, as most of the developments in addressing these challenges have been made in the context of MD. However, many principles and strategies to be discussed will also apply to MC. We highlight the most recent research findings that enrich or improve our mechanistic knowledge on wetting, scaling, and fouling in MD desalination. An important part of the mitigation strategies involves the application of membranes with special wetting properties, which is a relatively new field fueled by the recent advances in material science in understanding and developing surfaces with special wettability. However, we intend in this review to focus our discussion on the fundamental mechanisms instead of presenting a comprehensive survey of different membrane fabrication methods.

PORE WETTING

The most essential function of a membrane in MD and MC systems is to separate an aqueous stream from another liquid or gas stream in order to facilitate volatile component transport between the two streams. In MD and MC applications,

https://dx.doi.org/10.1021/acsestengg.0c00025
ACS EST Engg. 2021, 1, 117−140

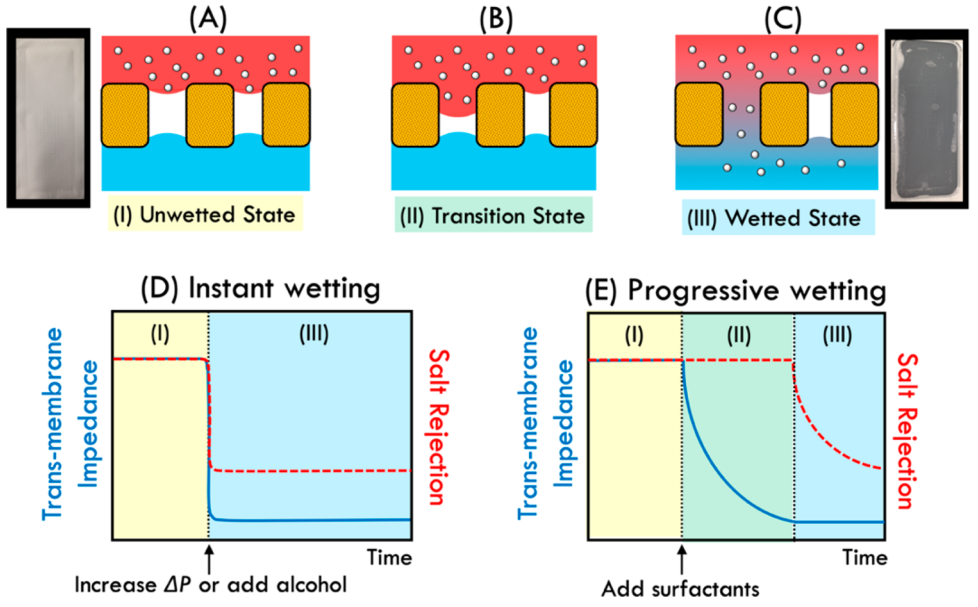

Figure 2. Various states in a wetting process. (A) Unwetted state: all pores are neither partially infiltrated nor fully penetrated. (B) Transition state: some pores are partially infiltrated, but no pore is fully penetrated. (C) Wetted state: some or all pores are fully penetrated. (D) Behavior (i.e., salt rejection and transmembrane impedance) of wetting induced by having a hydrostatic pressure exceeding the LEP. (E) Behavior of wetting induced by addition of surfactants.

membrane failure occurs when the liquid feed solution freely permeates through the membrane, a phenomena known as pore wetting.[27,28] In MD, wetting results in reduced salt rejection and, thus, contamination of the distillate stream;[2,39−42] whereas, in MC applications, wetting results in reduced mass-transfer and separation efficiencies.[43−45] In MD, the simplest and most common method for detecting wetting is measuring distillate electrical conductivity[46] (Figure 1A). The major limitation of this technique, however, is that it only detects wetting once the feed liquid has already fully penetrated at least a fraction of the membrane pores and contaminated the distillate.

Recently, in situ techniques based on single-frequency impedance[47] and light transmittance[48] have been developed to provide dynamic insights into the wetting process. With the technique based on single-frequency impedance, the air-filled pores separating the salty feed solution and distillate stream can be modeled as an equivalent circuit[49,50] (Figure 1A). The total impedance of this equivalent circuit decreases as the air-gap becomes progressively thinner due to the propagation of feed solution/air interface toward the distillate (Figure 1B). With the optical technique based on light transmittance (Figure 1A), the intensity of transmitted light is also dependent on the thickness of the air-filled pores (Figure 1B). The membrane transitions from being opaque when unwetted to being translucent when wetted.[48] While the wetting detection method is not the focus of this review, we want to emphasize that techniques are being actively developed to extract more information about the dynamic wetting phenomenon that has not been accessible by previous detection techniques that rely on the change of the distillate properties. The ability to unveil more information about the dynamic behavior of wetting is critical for enhancing our fundamental understanding of pore wetting.

Mechanism of Pore Wetting. *General Criterion of Pore Wetting.* Historically, pore wetting is explained based on force balance at the triple phase boundary with the help of an important concept called liquid entry pressure (LEP). LEP is the minimum hydrostatic pressure required to push the liquid into the membrane pores (for ideal cylindrical pores, entry is equivalent to penetration) and can be estimated using eq 1[51,52]

$$\mathrm{LEP} = -\frac{2B\gamma_L \cos\theta_0}{r} \tag{1}$$

where γ_L is the liquid surface tension, θ_0 is the intrinsic contact angle between the liquid and solid membrane material, r is the equivalent pore radius, and B is a geometric factor accounting for the noncylindrical nature of the membrane pore geometry ($B = 1$ for perfectly cylindrical pores). In general, reducing the surface tension of the feed solution reduces both γ_L and $\cos\theta_0$ (as θ_0 is also a function of γ_L), thus reducing LEP and facilitating pore wetting.[29,41,51−53] The general criterion for membrane pore wetting is that the transmembrane pressure, ΔP, exceeds LEP.[51,54]

$$\Delta P \geq \mathrm{LEP} \tag{2}$$

This criterion, as specified by the above inequality, applies well in most cases, provided the LEP can be accurately determined. If the membrane is composed of perfect cylindrical pores, the system will transition from an unwetted state (Figure 2A) to a wetted state (Figure 2C), as long as ΔP exceeds LEP, without going through any stable transition state (Figure 2B) observable by measuring the transmembrane impedance or optical transmittance. This abrupt transition from unwetted state to wetted state has been observed when (1) the hydraulic pressure of the feed solution undergoes a significant stepwise increase and (2) the surface tension of the feed solution is suddenly reduced by the addition of a large amount of water-miscible liquids such as alcohol. The absence of observable transition state (i.e., the nearly instantaneous wetting as shown in Figure 2D) is consistent with the kinetics of an expanding Poiseuille flow.[29,55,56] Assuming an ideal cylindrical pore, the depth of pore infiltration $l(t)$ can be estimated using eq 3[29]

https://dx.doi.org/10.1021/acsestengg.0c00025
ACS EST Engg. 2021, 1, 117−140

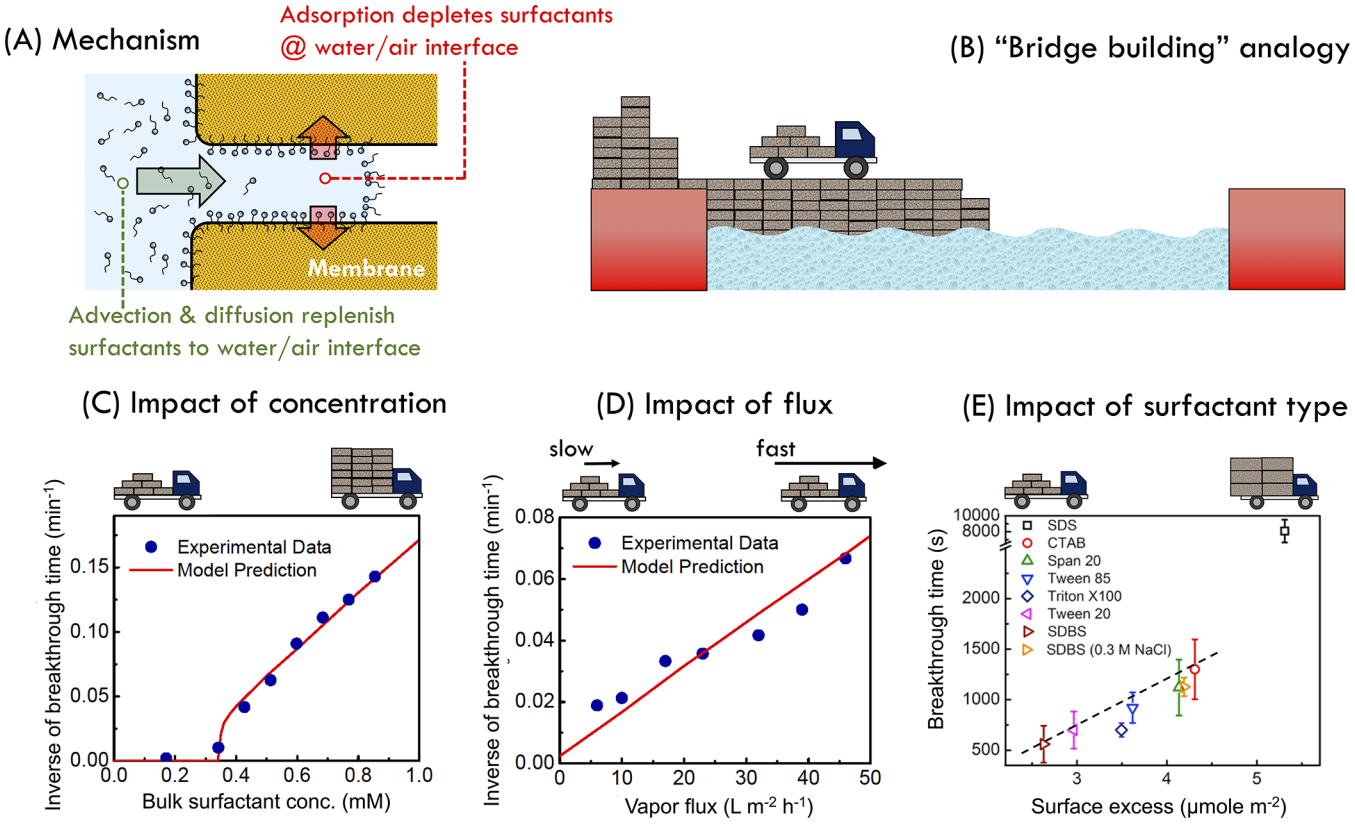

Figure 3. (A) Mechanism of surfactant-induced pore wetting featuring surfactants adsorption at the wetting frontier and the transport of surfactants from the bulk feed solution to the wetting frontier via advection and diffusion. (B) "Bridge building" analogy of the dynamic wetting model: passing the river (equivalent to "wicking through the pore") requires extending the bridge (equivalent to "saturating the pore surface surrounding the wetting frontier"). The impacts of (C) bulk surfactant concentration, (D) vapor flux, and (E) surfactant type, on the kinetics of wetting as quantified by breakthrough time or its inverse. The corresponding variables in the "bridge building" analogy are also given on the top of each panel. Adapted with permission from (C, D) ref 31 and (E) ref 32; Copyright 2018 and 2019 Elsevier, respectively.

$$l(t) = \sqrt{\frac{r^2}{4\mu}(\Delta P - \mathrm{LEP})t} \tag{3}$$

where r is the pore radius, μ is the dynamic viscosity of the feed liquid, t is time with $t = 0$ defined as the point that feed solution begins intruding into the membrane pores (see Wang et al.[29] for a more detailed derivation). Calculations based on eq 3 suggest that liquid penetration through a membrane pore typically takes only seconds, which explains the absence of an observable transition state.

Surfactant-Induced Wetting. What happens when the feed solution contains surfactants? Equation 2 suggests that wetting would occur just as in the case when low-surface-tension (LST) water-miscible liquid is added, except that we need a much lower concentration of surfactants, as they are very effective in reducing the liquid surface tension. However, both the impedance and optical transmittance-based techniques revealed that wetting induced by the addition of surfactants is transient, not instantaneous; that is, the transition state as illustrated in Figure 2B is observable for an extended period of time.[47,48] The observable transition state suggests that surfactant-induced wetting may have a very different mechanism as compared to that of wetting induced by increasing the ΔP or reducing the LEP via adding LST water-miscible liquids. The key to explaining the dynamic behavior of surfactant-induced wetting in MD is to understand that (1) surfactants readily adsorb onto a hydrophobic surface immersed in water and that (2) surfactants are very effective in reducing liquid surface tension, and thus it only requires a very low concentration of surfactants to reduce the LEP to be below the ΔP value.

The dynamic wetting behavior of surfactant-induced wetting has been recently elucidated and modeled,[29,31,32] and it is illustrated in Figure 3A. On the one hand, the fast adsorption of surfactants onto the hydrophobic membrane pore wall constantly removes surfactant from the solution near the water/air interface (i.e., the "wetting frontier"). On the other hand, advective transport due to water vapor flux and diffusive transport due to concentration gradient replenish surfactants from the feed solution (outside the pore) to the wetting frontier. The combination of the adsorption-driven depletion and transport-driven replenishment results in a surfactant concentration at the wetting frontier that is lower than the bulk concentration. The relevant LEP of the system should be calculated, not based on the surfactant concentration of the feed solution (in the bulk), but based on the surfactant concentration and the corresponding surface tension of the feed solution at the wetting frontier. In this context, eq 2 again becomes applicable, as the criterion for pore wetting, except that in this case the LEP of the wetting frontier, not of the bulk feed solution, should be compared with ΔP.

The theory presented above explains why instantaneous wetting does not occur even if LEP calculated from the bulk surfactant concentration is lower than ΔP. However, pore wetting still occurs gradually, because the pore wall surface has a limited capability for surfactant adsorption. When the wetted

https://dx.doi.org/10.1021/acsestengg.0c00025
ACS EST Engg. 2021, 1, 117−140

surface of the pore is saturated, adsorptive depletion of surfactants no longer occurs, which leads to the increase in the surfactant concentration at the wetting frontier and, correspondingly, to the reduction of the surface tension and LEP. Once the LEP becomes lower than ΔP, wetting occurs, and the wetting frontier propagates toward the distillate. This forward propagation exposes a new region of the pore to the feed solution, which again enables rapid adsorption of surfactants to increase the LEP beyond ΔP until that new region is again saturated with surfactants. Such a process of adsorption, saturation, and forward propagation of the wetting frontier repeats itself and results in the experimentally observed transient wetting. While this phenomenon is described here as a stepwise process to facilitate understanding, it is continuous in a real process.

It may be helpful to illustrate this new model for surfactant-induced wetting with an interesting analogy of "bridge building" (Figure 3B). To build a bridge (i.e., for the feed solution to fully penetrate a hydrophobic pore), bricks (i.e., surfactant molecules) must be transported to the bridge frontier and laid there to further extend the bridge. The brick-laying process (i.e., the adsorption of surfactants to the pore wall at frontier) is very fast. Therefore, the kinetics of the bridge-building process is limited by how fast the bricks are transported to the bridge frontier. This bridge building analogy leads to several important implications. For example, if the brick-transporting truck carries more bricks per truck, which is equivalent to having a higher feed concentration of surfactants (as the advection term is proportional to concentration), the bridge building (pore wetting) process is faster (Figure 3C; note that, if the bulk surfactant concentration is too low, wetting does not occur, because ΔP is lower than the LEP of the bulk solution). In addition, if the truck moves faster, which is equivalent to having a higher flux (as the advection term is proportional to flow velocity), the bridge building (pore wetting) process is also faster (Figure 3D). These two dependences of wetting kinetics on experimental conditions have been shown experimentally and predicted accurately by the dynamic wetting model.[31,32]

The most interesting conclusion from the model regards how the surfactant type affects the wetting kinetics. The bridge building analogy suggests that, if the bricks are bigger (primarily, longer), the bridge will be extended faster provided (1) all trucks move at the same speed and (2) each truck carries the same number of bricks. Equivalently, the dynamic wetting model predicts that "bigger" surfactants will lead to faster pore wetting (i.e., shorter breakthrough time), which has also been experimentally confirmed[31,32] (Figure 3E). Here, the size of the surfactants can be quantified using surface excess concentration Γ, which can be evaluated using the Gibbs adsorption isotherm.[57−59] Specifically, a very nice linear correlation has been experimentally shown between the surface excess concentration and the breakthrough time for a series of surfactants of different charges (Figure 3E, except for sodium dodecyl sulfate, for which diffusion has an important contribution to transport. See a detailed explanation in the work of Wang et. al.[32]). This experimentally validated model emphasizes the "size" of surfactants as a key property that influences how efficiently different surfactants induce wetting (assuming the same molar concentration), which is in contrast to the previous understanding that focused on the interaction between the surfactant and the pore surface.[30,60] According to the dynamic wetting model, the surfactant-pore surface interaction is irrelevant to the kinetics of pore wetting, because adsorption, which is much faster than transport of surfactants to the frontier, is not the rate-limiting step.

The dynamic model for surfactant-induced wetting is the first quantitative model for predicting the kinetics of surfactant-induced wetting. The model, which provides a satisfactory fitting to the experimental data from multiple dimensions, is based on the assumption that wetting occurs only when the ΔP exceeds the LEP at the wetting frontier. Another plausible mechanism for propagation of the wetting frontier is via the "autophilic effect", that is, the surfactants can adsorb onto the unwetted part of the surface ahead of the triple phase boundary and thereby reduce the surface energy of the unwetted part of the surface near the wetting frontier, making it hydrophilic.[61,62] As a result, the propagation of the liquid−air interface toward the distillate is spontaneous and can occur without applied pressure. The "autophilic" explanation, however, has challenges in explaining why there exists a minimum bulk surfactant concentration below which wetting does not occur (Figure 3A). Moreover, the subtle impact of ΔP on the wetting kinetics, which has been experimentally validated, also appears to confirm the assumed wetting criterion based on comparing the ΔP and the LEP. Whether an autophilic effect does play an important role in surfactant-induced wetting requires further investigation. However, even assuming an autophilic effect is important, because the adsorption of surfactants onto a hydrophobic surface immersed in water is highly energetically favorable, we speculate that the autophilic effect can only exert its contribution when a wetted pore surface is saturated with surfactants. In other words, the bridge building analogy and the kinetic model of pore wetting focusing on the critical role of surfactant transport should apply regardless of the exact mechanism of frontier propagation.

Wetting Mitigation Strategies. *Pretreatments.* There are limited pretreatment techniques that may mitigate membrane pore wetting. For example, physical pretreatments such as microfiltration (MF), ultrafiltration (UF), or nanofiltration (NF) can effectively remove amphiphilic proteins that may eventually wet the pores of a hydrophobic membrane.[63,64] However, they cannot mitigate pore wetting induced by surfactants or LST water-miscible liquids. Surfactants can be removed from solution via ion exchange,[65] coagulation,[66,67] floatation or foam fractionation,[68−70] or biodegradation.[71,72] While some of the aforementioned pretreatment methods have not yet been tested for MD or MC and a knowledge gap exists in matching the appropriate pretreatment method given a real water application, some studies have shown promise in using these pretreatment strategies for MD and MC. For example, dispersing bubbles into a surfactant-containing feed solution from the textile industry formed floating foams that removed surfactants from the bulk solution. This foam fractionation pretreatment in turn eliminated the surfactant-induced wetting that had previously occurred in the downstream MD process.[70] In another study, MC used for ammonia stripping from a model wastewater stream was plagued by eventual wetting due to amphiphilic protein molecules. After the integration of the MC process with a microfiltration or ultrafiltration pretreatment, the tested poly(tetrafluorethylene) (PTFE) and polypropylene (PP) membranes realized a twofold and fourfold increase in the ammonia mass-transfer coefficients, respectively, and membrane wetting was never observed throughout the duration of the 30 h experiment.[64] For a feed solution containing LST water-miscible liquids as often

https://dx.doi.org/10.1021/acsestengg.0c00025
ACS EST Engg. 2021, 1, 117−140

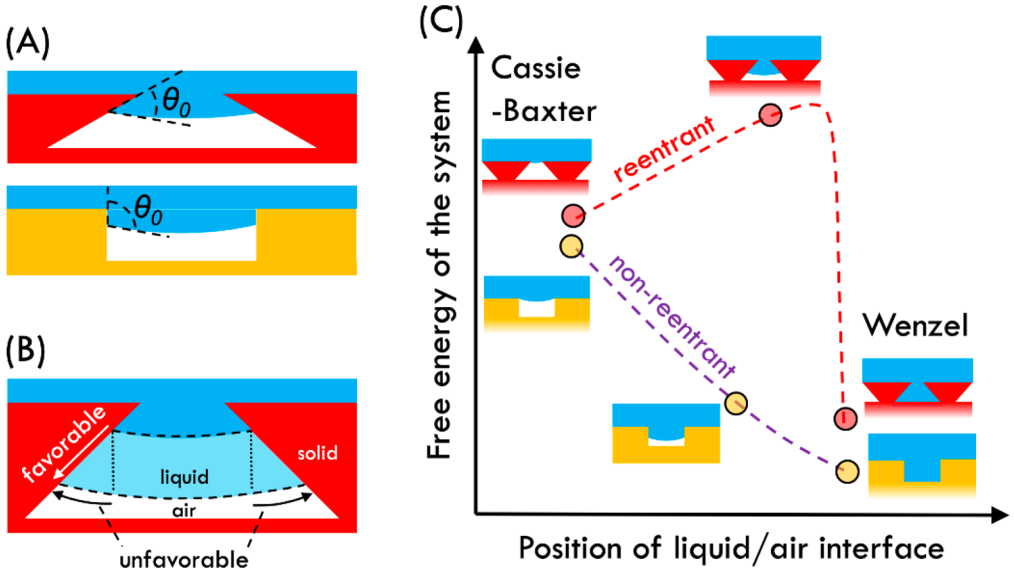

Figure 4. (A) Local intrinsic contact angles at the local triple-phase boundary for a reentrant structure (top) and a nonreentrant structure (bottom). (B) Illustration of how a liquid intrusion into a pore with reentrant geometry would change the contact area of the liquid/solid and liquid/air interfaces. (C) Free energy profile as a function of the position of the liquid/air interface for pores with reentrant and nonreentrant geometries.

encountered in MC, no viable pretreatment exists for wetting mitigation, as the removal of the wetting agent is precisely the technical goal of MC itself. In general, if the feedwater has a composition that may promote pore wetting in MD or MC, options to mitigate wetting via pretreatment are fairly limited. Therefore, a different approach based on developing a wetting-resistant membrane is needed for more versatile and robust wetting mitigation.

Omniphobic Membranes. Because all wetting processes, whether induced by surfactants or alcohol, follow the same principle described by eq 2, we can develop membranes that resist wetting by LST liquids as a strategy for wetting mitigation. Membranes that are resistant to wetting by LST liquids, such as oil, are called oleophobic membranes. In most cases, oleophobic membranes are also hydrophobic and thus are referred to as amphiphobic or omniphobic membranes.[73,74] Without specifying the medium, the definitions of wetting property assume air as the medium. Strictly speaking, omniphobicity literally refers to resistance to wetting by all liquids, whereas amphiphobicity refers to wetting resistance to both water and oil. The difference between the two concepts is more quantitative than qualitative. For instance, a membrane may be referred to as amphiphobic if it is resistant to wetting by mineral oil ($\gamma \approx 30$ mN m^{-1}) but not by ethanol ($\gamma \approx 22$ mN m^{-1}) and *n*-decane ($\gamma \approx 24$ mN m^{-1}). Therefore, we use omniphobic membranes here to refer broadly to membranes with resistance to wetting by LST liquids.

The development of an omniphobic membrane for MD application was first reported in 2014[28] and has since attracted extensive research interest.[73−82] For example, omniphobic membranes have shown promising wetting resistance in treating produced water from the oil and gas[73,74] and coking industries.[76] However, the fundamental mechanism of achieving omniphobicity had been elucidated by the material science community several years earlier.[83−86] Without going through the theoretical derivation (interested readers are referred to these publications[83,84]), here we summarize the criteria for developing omniphobic membranes and the basic principle behind such criteria.

The two major criteria for making an omniphobic membrane or, more generally, an omniphobic surface, are that (1) the material has a low surface energy and (2) the surface has a reentrant texture. The first criterion is shared by both hydrophobic and omniphobic membranes and is often met by using fluoro-polymers and surface modifiers, which are known to be of low surface energy and chemically relatively stable. In describing the wetting state of a general textured substrate surface, if the liquid is in full contact with the substrate, the system is in a Wenzel state; if the liquid is supported by a composite surface comprising the protrusions of the solid substrate and the air pockets between these protrusions, the system is in a Cassie−Baxter state.

In the context of membrane wetting, the composite interface at the wetting frontier that comprises the membrane pores and the solid surface itself envelopes the aforementioned "surface texture". The Cassie−Baxter state corresponds to the unwetted state depicted in Figure 2A, when the LEP at the wetting frontier is high enough to deter any liquid infiltration into the membrane pores toward the direction of the distillate stream. Likewise, the Wenzel state corresponds to the wetted state depicted in Figure 2C, when the LEP at the wetting frontier satisfies the condition stipulated by eq 2 and thus results in pore wetting. To prevent wetting of any degree, the wetting frontier needs to be maintained in a Cassie−Baxter state at the membrane surface. The thermodynamics of wetting suggests that the maintenance of a Cassie−Baxter state for high-surface-tension liquids, such as water, can be achieved as long as the porous membrane is made of low-surface-energy materials.[75,87] However, it also suggests that the Cassie−Baxter state is not stable (i.e., it has a higher free energy than that of the Wenzel state) if the surface tension of the liquid is sufficiently low. Here comes the important role of the reentrant texture (the second criterion) that sustains a metastable Cassie−Baxter state.

https://dx.doi.org/10.1021/acsestengg.0c00025
ACS EST Engg. 2021, 1, 117−140

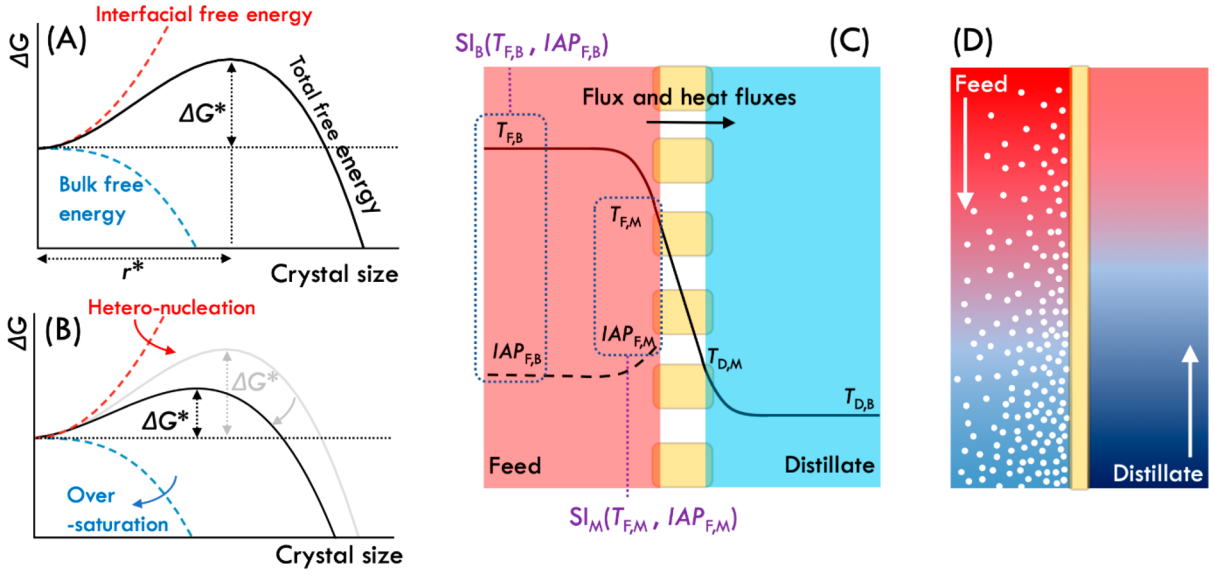

Figure 5. (A) CNT considering contributions from both reduction in bulk free energy and increase in interfacial free energy. (B) Reducing free energy barrier for nucleation via (1) heteronucleation and (2) oversaturation. (C) Local spatial distribution of temperature and salt concentration in the direction normal to the membrane, featuring temperature and concentration polarizations. Specifically, *T*, IAP, and SI represent temperature, ion activity product, and saturation index, respectively; the first subscripts, F and D, denote the properties of the feed solution and distillate, respectively; the second subscripts, B and M, denote the properties in the bulk and at the membrane surface, respectively. (D) Spatial distribution of temperature (represented by color—red symbolizing high temperature and blue symbolizing low temperature) and salt concentration (represented by density of white dots) in the MD module.

A reentrant texture is a concave topography in which the cross-sectional area of a pore increases with the depth of the pore. A classic reentrant texture is an array of inverted cones. Figure 4A shows the cross-section of space between two inverted cones (top) versus that between two cylinders (bottom). The requirement of a reentrant texture to maintain a Cassie—Baxter state with even LST liquids can be explained using both force balance and free energy analysis. Without a reentrant texture, the maintenance of a Cassie—Baxter state requires that local contact angle be higher than 90° (Figure 4A bottom), which can be satisfied if the solid material constituting the pores has a low surface energy and the liquid has high surface tension (e.g., water). However, with LST liquids, a local contact angle does not exceed 90° even with solid material with low surface energy. In this case, the Cassie—Baxter state can only be maintained with a reentrant texture with which the local contact angle can be lower than 90° (Figure 4A top).

The necessity of reentrant texture for achieving omniphobicity can also be elucidated from the perspective of free energy. When liquid infiltrates into a pore, part of the solid/air interface is replaced by a solid/liquid interface (Figure 4B). If the solid surface has a low surface energy and the liquid has a high surface tension, the replacement of the solid/air interface by a solid/liquid interface is energetically unfavorable, which explains the stable Cassie—Baxter state for water contacting a hydrophobic membrane. When an LST liquid is considered, this replacement is energetically favorable even if the pore is made of low-surface-energy materials. However, with and only with reentrant texture, the liquid infiltration expands the liquid/air interface, which is energetically unfavorable. If the unfavorable expansion of the liquid/air interface outweighs the favorable expansion of the solid/liquid interface, a free energy barrier would exist in the process of the transition from the Cassie—Baxter state to the Wenzel state when the pore is fully infiltrated (Figure 4C). Therefore, a metastable Cassie—Baxter state can exist with LST liquid in the presence of a reentrant structure. On the contrary, the transition from the Cassie—Baxter state to the Wenzel state would monotonically reduce the free energy if the system does not have a reentrant texture that promotes expansion of the liquid/air interface upon pore infiltration (Figure 4C).

While inverted cones are convenient models for illustrating a reentrant structure, they are not a practical structure to engineer on a membrane. Instead, fibers from electrospinning or nanoparticles from spraying or solution-phase adsorption are used to construct the reentrant texture for omniphobic membranes.[74−76,78] Recent studies also find that omniphobic membranes can be obtained by simple chemical modification to reduce the surface energy of commercial hydrophobic membranes, which suggests that the structure of some commercial hydrophobic membranes is already reentrant.[88] It also suggests that whether a Cassie—Baxter state can be maintained depends on the intricate interplay between liquid surface tension, surface energy of the solid, and the pore geometry. If the membrane is made of material of lower surface energy and/or has a more robust reentrant structure (the readers can refer to ref 84 for the theory about the robustness of oleophobicity), the membrane may become "more omniphobic" and can sustain stable MD performance with a feed solution of a lower surface tension. In an extreme case with a doubly reentrant structure, even a surface of high surface energy (e.g., silica) can be omniphobic.[89] As mentioned above, this article is not focusing on membrane fabrication methods. Therefore, readers who are interested in fabricating omniphobic membranes can refer to these review papers.[38,82,90]

MINERAL SCALING

Mineral scaling is extremely relevant to MD, as its most opportunistic applications are for treating hypersaline indus-

https://dx.doi.org/10.1021/acsestengg.0c00025
ACS EST Engg. 2021, 1, 117−140

trial wastewater where reverse osmosis (RO) is not feasible.[1] Depending on the pretreatment methods used, hypersaline wastewaters often contain ions that form sparingly soluble minerals (i.e., sulfates, carbonates, and silicates).[91] During MD, these compounds are concentrated as water evaporates, which eventually leads to the development of a precipitated layer of mineral crystals on the membrane surface, also known as mineral scaling.[34] Mineral scaling can occur via the deposition of precipitates formed in the bulk solution or direct nucleation and growth of precipitates on the membrane surface. In either case, scaling reduces process efficiency or leads to process failure, and it must be properly addressed to maximize the potential for applying MD toward addressing broader water treatment challenges.[92]

Mineral scaling is mostly detected by monitoring the water vapor flux over time.[93,94] Typically, an appreciable decrease in water vapor flux is indicative of scaling, as the scaling layer blocks the membrane pores. Although this method involves a straightforward indicator that is directly relevant to membrane performance, it only allows scaling to be detected after much of the membrane surface has been covered and provides little information regarding the growth kinetics, spatial distribution, morphology, and composition of the scale layer. Ex situ membrane autopsy has helped elucidate scaling mechanisms and how they relate to operation parameters and membrane characteristics. A suite of standard material characterization techniques has been used for membrane autopsy, including scanning electron microscopy (SEM) with energy-dispersive X-ray spectroscopy (EDS), Fourier-transformed infrared (FTIR) spectroscopy, atomic force microscopy (AFM), X-ray diffraction (XRD), and X-ray photoelectron spectroscopy (XPS).[95−97]

There has also been some progress on the development of in situ scaling observation techniques. For example, optical coherence tomography (OCT) has revealed that hardly any scaling particles were visible before the vapor flux decline.[98,99] Also, a laser-based optical technique has been used to measure the concentration profiles of metal chloride salts in the MD feed solution near the membrane surface.[100] However, more powerful and easy-to-implement in situ scaling detection methods are still in need to better elucidate the dynamics of scaling, especially during the early stages of crystal growth.

Mechanism of Scaling. *General Scaling Criterion.* Mineral precipitates form when the species' concentration product exceeds its solubility product. Like other mineralization processes occurring in nature, the formation of mineral scales in membrane desalination follows the theories established under the framework of classic nucleation theory (CNT).[101] The CNT describes the change of free energy (ΔG) associated with the formation of a nascent cluster of a new solid phase (from ions), which is expressed as the sum of two terms (eq 4, Figure 5A)[102]

$$\Delta G = -n\Delta\mu + A\gamma_{ln} \tag{4}$$

where n is the number of ions in a cluster, $\Delta\mu$ refers to the chemical potential difference of the ions between their solution phase and solid phase, A is the surface area of the cluster, and γ_{ln} refers to the interfacial energy between the liquid and the nucleus. The first term on the right side of eq 4 represents the energy change associated with the formation of bulk mineral from n growth units (i.e., bulk free energy), which is always negative under supersaturated conditions; the second term regards the energy gain (penalty) associated with increasing the interfacial area (i.e., interfacial free energy). Assuming a spherical nucleus of radius r, the change in the free energy during homogeneous nucleation is given by eqs 5 and (6)[102]

$$\Delta G_{hom}(r) = -\frac{4}{3}\frac{N_A\pi\Delta\mu}{v_m}r^3 + 4\pi\gamma_{ln}r^2 \tag{5}$$

where N_A and v_m are the Avogadro number and molar volume, respectively. The chemical potential difference $\Delta\mu$ is dependent on the degree of oversaturation

$$\Delta\mu = k_B T \ln\left(\frac{IAP}{K_{sp}}\right) \tag{6}$$

where k_B is the Boltzmann constant, T is the absolute temperature, IAP is the ion activity product, and K_{sp} is the equilibrium constant (or solubility product). As shown in Figure 5A, $\Delta G_{hom}(r)$ reaches a maximum value (ΔG^*) when the mineral nucleus grows to a critical size r^*. Only the nuclei with sizes larger than r^* can evolve into thermodynamically stable minerals. Therefore, ΔG^* represents the height of the energy barrier of mineral nucleation.

Equations 5 and (6) bridge the degree of saturation of the feed solutions to the thermodynamic energy barrier of scale formation. Saturation index (SI) is often used in the literature to quantify the scaling potential of the feedwater in membrane desalination.[95,103−106] While there are multiple definitions of SI in the literature (it has been defined as $\ln(IAP/K_{sp})$, $\log_{10}(IAP/K_{sp})$, or (IAP/K_{sp})), the SI based on all these definitions consistently increases as the solution becomes more concentrated. With an increase of SI, $\Delta\mu$ increases (according to eq 6) and ΔG decreases (according eq 4 or (5)), resulting in a lower nucleation energy barrier (ΔG^* in Figure 5B) and easier mineral formation.

For heterogeneous nucleation, which could take place on membrane surfaces or foreign particles in the bulk solution, the interfacial energy at the liquid-substrate (γ_{ls}), substrate-nucleus (γ_{sm}), and liquid-nucleus (γ_{ls}) interfaces needs to be considered.[102] The presence of a substrate surface decreases the interfacial free energy (Figure 5C), which also leads to a reduction of the nucleation energy barrier. The energy barrier of heterogeneous nucleation (ΔG^*_{het}) relates to that of homogeneous nucleation (ΔG^*_{hom}) by a correction factor called the wetting function $f(\theta_{n/w})$[107]

$$\Delta G^*_{het} = f(\theta_{n/w})\Delta G^*_{hom} = \frac{1}{4}(1 - \cos\theta_{n/w})^2 \times (2 + \cos\theta_{n/w})\Delta G^*_{hom} \tag{7}$$

where $\theta_{n/w}$ is the contact angle of a nucleus (assuming a spherical cap geometry) on the substrate in water as the medium (we note that θ_n should not be misinterpreted as the in-air water contact angle of the membrane substrate, which will be denoted as θ_w). Because the morphology of the nucleus is determined by the crystal structure and not necessarily a spherical cap, $\theta_{n/w}$ is more of a hypothetic metric to quantify the interaction between the mineral nucleus and the substrate based on the Young equation.

$$\cos\theta_{n/w} = \frac{\gamma_{ls} - \gamma_{sn}}{\gamma_{ln}} \tag{8}$$

Most membrane substrates in MD are nonpolar polymers that do not have polar interaction (also called acid−base

https://dx.doi.org/10.1021/acsestengg.0c00025
ACS EST Engg. 2021, 1, 117−140

interaction according to Van Oss[108]). Therefore, the γ_{ls} and γ_{sm} terms in eq 8 can be written as[109]

$$\gamma_{ls} = \gamma_l + \gamma_s - 2\sqrt{\gamma_l^D \gamma_s^D} \quad (9)$$

and

$$\gamma_{sn} = \gamma_s + \gamma_n - 2\sqrt{\gamma_s^D \gamma_n^D} \quad (10)$$

where γ_l, γ_s, and γ_n are the surface energy of the liquid, substrate, and nucleus, respectively, and γ_l^D, γ_s^D, and γ_n^D are the contributions of dispersion force (also called Lifshitz-van der Waals interaction by Van Oss) to the surface energy of the liquid, substrate, and nucleus, respectively. Considering eqs 9, (10), and the equality of $\gamma_s \approx \gamma_s^D$ for a nonpolar substrate, eq 8 can be rewritten as

$$\cos\theta_{n/w} = \frac{\gamma_l - \gamma_n - 2\sqrt{\gamma_s}\left(\sqrt{\gamma_l^D} - \sqrt{\gamma_n^D}\right)}{\gamma_{ln}} \quad (11)$$

Depending on the temperature, γ_l^D is slightly higher than 20 mN m^{-1} for water. Without known exception, γ_n^D is always larger than γ_l^D (e.g., $\gamma_n^D \approx 37$ mN m^{-1} for silica[110] and $\gamma_n^D \approx 47$ mN m^{-1} for gypsum[111]). Therefore, $\sqrt{\gamma_l^D} - \sqrt{\gamma_n^D}$ is negative, and thus $\cos\theta_{n/w}$ positively correlates with γ_s. In other words, as the substrate becomes more hydrophobic (as a result of reduced γ_s), the contact angle $\theta_{n/w}$ in eq 7 also increases (as $\cos\theta_{n/w}$ decreases).

The value of $f(\theta_{n/w})$ in eq 7 ranges between 0 and 1 when $\theta_{n/w}$ changes from 0 to π, consistent with the above discussion that ΔG^*_{het} is lower than ΔG^*_{hom}. The occurrence of heterogeneous nucleation is more favorable than homogeneous nucleation, and thus the presence of a surface (e.g., membrane) promotes scale formation. While ΔG^*_{hom} is a constant at a specific temperature and SI, a difference in membrane materials may result in different energy barriers for heterogeneous nucleation. This partially lays the foundation of fabricating scaling-resistant membranes by tuning membrane surface properties to inhibit heterogeneous nucleation.[95,96,103,112,113]

The CNT theory also provides insights into the change of scaling potential due to the concentration and temperature polarization in an MD process. Concentration polarization is a phenomenon in which solutes accumulate within a boundary layer near the membrane surface as a result of the advective transport of solute toward a nonpermeable boundary and the back-diffusion due to concentration gradient (Figure 5C). Concentration polarization leads to a higher IAP at the membrane surface than in the bulk, which consequently affects the SI at the membrane surface. Besides, temperature polarization refers to a decrease of feedwater temperature from the bulk to the membrane surface due to the limited heat transfer rate across the boundary layer (Figure 5C).[114] Temperature polarization reduces the temperature at the membrane surface as compared to that of the bulk and, also, thereby alters SI via changing the temperature-dependent K_{sp}. For example, the solubility of NaCl and silica is enhanced with increased temperature,[115,116] whereas an inverse correlation between temperature and solubility was reported for calcite ($CaCO_3$) and Na_2SO_4.[116−118] There are also minerals for which the correlation between solubility and temperature is not monotonic. For example, the solubility of gypsum ($CaSO_4 \cdot 2H_2O$) peaks at ~40 °C.[119] The combination of the effects of concentration and temperature polarization may result in an SI at the membrane surface that differs substantially from that in the bulk, which adds to the impact of heterogeneous nucleation.

In practical MD membrane modules, the mass and heat transfer across the membrane also causes spatiotemporal variations in temperature and solute concentration along the channels. As more water is recovered, the solute concentration in the feed stream gradually increases. However, such an increase in solute concentration occurs more temporally than spatially, as the maximum water recovery per pass is limited to a few percent.[10,11] Therefore, the scaling potential always increases over time, as water recovery increases. In contrast, the spatial distribution of temperature along the module is substantial due to the large amount of latent heat transfer associated with vapor transfer (Figure 5D). Consequently, the dependence of scaling potential on the module position (at a given moment) is strongly dependent on the type of correlation between solubility and temperature.

Understanding Mineral Scaling Beyond CNT. Scaling in MD is a rather complex process that involves multiple fundamental phenomena in parallel and/or in sequence. These phenomena include, but are not limited to, ion transport, nucleation, precipitate growth, particle deposition, and adhesion. While understanding CNT and concentration/temperature polarization are important to understand scaling, knowledge gaps still exist to precisely predict long-term membrane performance in MD subject to mineral scaling. Typically, membrane performance refers to vapor flux and salt rejection. These two metrics can be easily measured and are most relevant in practical operation. A widely investigated parameter that is particularly relevant to understanding the kinetics of mineral scaling is the induction time. The relevant induction time is the period from process initiation to the onset of irreversible flux decline due to mineral scaling. Notably, the induction time of flux decline caused by mineral scaling in membrane desalination is fundamentally distinct from the induction time of scale formation, which refers to the time between the generation of a supersaturated solution and the formation of the first nuclei.[120] The induction of scale formation, a physicochemical phenomenon, is believed to occur much earlier than the onset of flux decline, an operational phenomenon. The relationship between those two "inductions" is still unknown and requires further investigation.

The roles of heterogeneous and homogeneous nucleation in regulating scaling behavior in MD have not been fully understood. Although heterogeneous nucleation occurs more favorably than homogeneous nucleation due to the reduction of the energy barrier, both may take place in an MD process, especially considering the high salinity of the feedwater. The contributions of the heterogeneous and homogeneous nucleations to mineral scaling are difficult to quantify separately, but a better understanding of their respective contributions is essential for predicting scaling kinetics and developing scaling mitigation strategies. For example, homogeneous silica nucleation has been shown to play a dominant role in initiating the decline of water vapor flux, while heterogeneous silica nucleation facilitates the membrane pore blockage.[121] In another study, filtering a supersaturated calcium sulfate feed solution to remove homogeneously precipitated crystals proved to limit the rate of flux decline due to scaling.[122] If that is proven generally true for all

https://dx.doi.org/10.1021/acsestengg.0c00025
ACS EST Engg. 2021, 1, 117−140

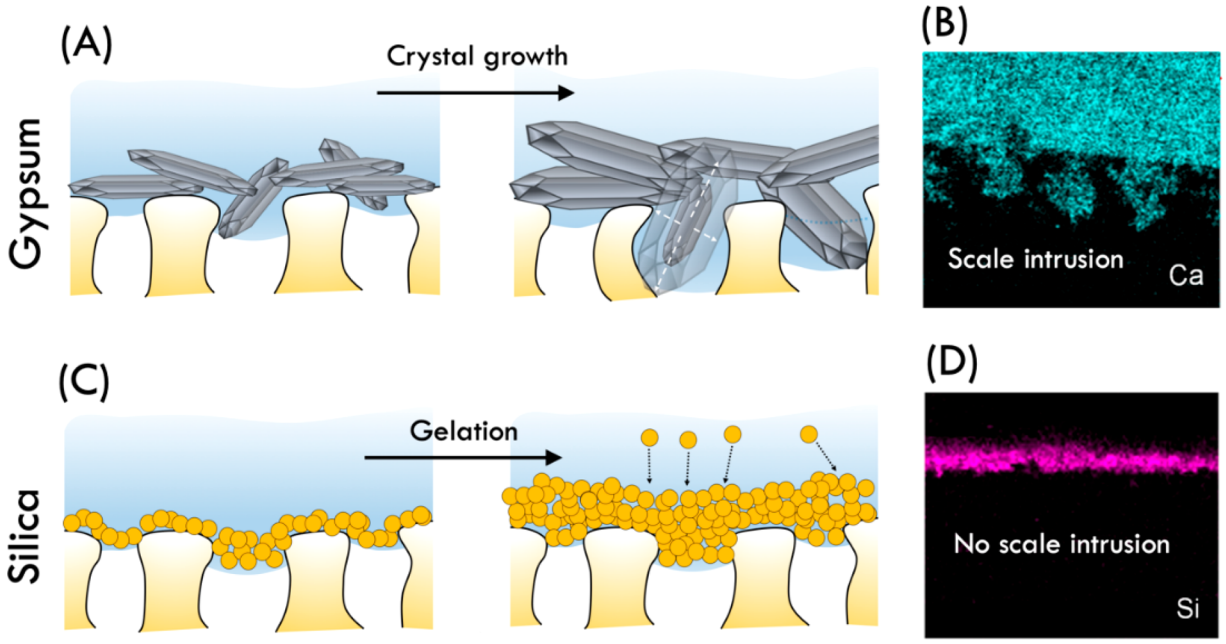

Figure 6. (A) Mechanism of gypsum scaling-induced wetting via pore deformation under crystallization pressure. (B) SEM-EDS images showing gypsum intrusion into the membrane pores. (C) Silica scaling via gelation of silica nanoparticles. (D) SEM-EDS images showing the absence of silica intrusion into membrane pores. Adapted with permission from ref 35.

common scaling species, the inhibition of precipitation in the bulk solution and the abatement of precipitate deposition onto the membrane surface will be more effective in mitigating membrane scaling than hindering heterogeneous nucleation by altering membrane surface properties.

In addition, to develop an improved general framework for understanding mineral scaling in MD, we also need to acquire a better understanding of the species-dependent behavior of MD scaling. Different types of scaling could have distinct mechanisms of precipitate formation at the molecular level and different consequences in their macroscopic scaling behavior (Figure 6).[35] Some scales, including gypsum, calcite, and NaCl, are formed via a crystallization process (Figure 6A). In the case of gypsum scaling, it has been shown that crystal growth causes scaling intrusion (into the pores) and pore deformation (Figure 6B). The pore deformation eventually leads to membrane wetting, as LEP is reduced with larger deformed pores.[35,123,124] In contrast, silica scaling results from the polymerization of silicic acid followed by gelation (Figure 6C).[121] Consequently, it does not result in the same intrusion and pore deformation phenomena observed in gypsum scaling (Figure 6D). In consequence, MD with silica scaling is only plagued with flux decline but not membrane wetting. Therefore, mineral scaling formed by crystallization should receive special attention in MD desalination of wastewater with mixed salts, due to its potential for causing membrane wetting. It would be valuable to evaluate whether wetting-resistant membranes, such as those described above, are also effective to mitigate membrane wetting caused by inorganic scaling.

Scaling Mitigation Strategies. *Pretreatments.* The use of antiscalants is the most straightforward approach of controlling mineral scaling in membrane desalination including MD.[125−134] For example, organic phosphonate derivatives were found to mitigate the precipitation of calcium scales in the MD treatment of seawater RO brine,[133] while the application of a proprietary polymeric compound was reported to retard calcite scaling in MD with coal seam gas RO brine as the feedwater.[135] Additionally, carboxylic-based polymeric molecules also inhibit the nucleation of calcite and gypsum in MD.[128] Antiscalants typically serve as nucleation inhibitors that hinder homogeneous nucleation in feed solutions. The two major mechanisms that are likely responsible for scaling inhibition are (1) the formation of soluble complexes in the bulk solution, which decreases the SI by reducing availability of the "free" ions for precipitation, and (2) the direct adsorption onto the nuclei surface, which retards the mineral growth.[9,37] Antiscalants that are widely used in industry are weak acids such as phosphonate derivatives and polymeric molecules anchored with carboxylic groups. Under near-neutral conditions of desalination, such antiscalants are partially or fully deprotonated, exposing negative active sites that are able to form complexes with multivalent cations in the solution.[136−139] For example, poly(acrylate acid) (PAA), a carboxylic derivative polymer with pK_a of 4.4,[140] is highly deprotonated at approximately the pH of 7 and may strongly chelate with Ca^{2+} to reduce its activity for precipitating with CO_3^{2-} or SO_4^{2-} to form calcite or gypsum.[141,142] However, this complex formation mechanism is challenged by the fact that the antiscalants can be highly effective at a very low concentration—much lower than the concentration of Ca^{2+} stoichiometrically.[143,144]

Another possible mechanism for the role of antiscalants in scaling inhibition is the adsorption of antiscalant molecules onto the surface of crystal nuclei via either electrostatic interaction or ligand exchange.[142−147] Adsorption of antiscalants may contribute to scaling mitigation in two different ways. First, the adsorption of antiscalants on the nuclei surface increases the interfacial free energy at the liquid-nucleus interface,[148] thereby increasing the energy barrier of nucleation according to the CNT as discussed in the previous section. This consequently reduces the nucleation rate and extends the induction time of scaling.[128,145,148] Second, the attachment of antiscalants reduces the active nuclei surface area for crystal growth.[149,150]

https://dx.doi.org/10.1021/acsestengg.0c00025
ACS EST Engg. 2021, 1, 117−140

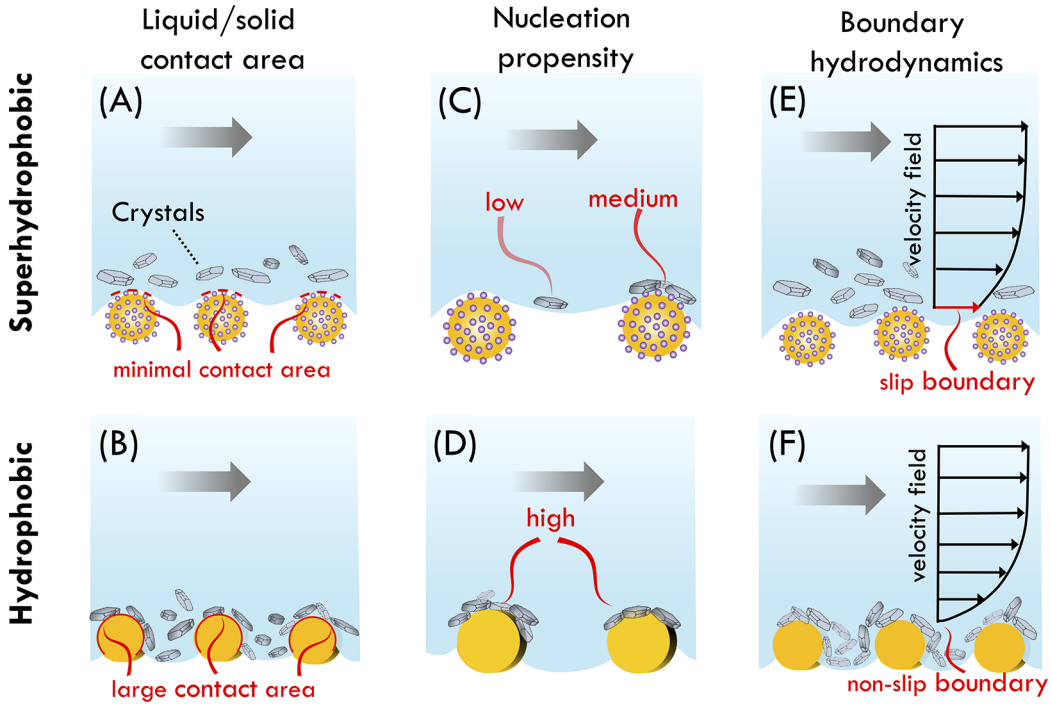

Figure 7. Possible mechanisms for the scaling mitigation with superhydrophobic membranes (top) relative to conventional hydrophobic membranes (bottom). (A, B) Reducing solid/liquid contact area. (C, D) Reducing nucleation propensity by reducing surface energy. (E, F) Enhancing boundary cross-flow and eliminating stagnant zones in a partially wetted pore. Adapted with permission from ref 96.

Besides the use of antiscalants, other strategies have been applied for the mitigation of mineral scaling in MD. Coagulation and softening are common approaches to remove scalants from the feedwater prior to the MD process.[151] For example, precipitative softening has been shown to reduce the concentrations of several scale-forming species (e.g., Ca^{2+}, Sr^{2+}, and silica) in produced water from shale oil and gas production, decreasing the corresponding SI of sparingly soluble salts such as calcite, silica, and strontianite ($SrCO_3$).[152] This resulted in the effective mitigation of mineral scaling and improved water recovery in the subsequent MD process. In addition to these chemical-based pretreatments, nanofiltration has been explored for softening the feedwater before MD to mitigate scaling.[33]

Superhydrophobic Membranes. The use of a superhydrophobic membrane can complement the pretreatment strategies and contribute to the overall reduction in membrane scaling potential.[95,96,112,113,153,154] Superhydrophobic membranes are characterized by their extreme nonwetting property. In general, a surface is typically considered superhydrophobic if (1) the static water contact angle is higher than 150° and (2) the sliding angle is below 10° (alternatively, contact angle hysteresis, which is the difference between the advancing and receding contact angles, can be used instead of a sliding angle). In the MD literature, superhydrophobic membranes are sometimes also referred to as slippery membranes.[1,112,113] Membrane superhydrophobicity is achieved by minimizing the liquid–solid contact area via introducing rough, and preferably hierarchical, surface texture. If we denote ϕ as the areal fraction of a solid–liquid interface over the entire liquid interface (with both solid and air), the apparent water contact angle $\theta_{w,A}$ (i.e., the water contact angle actually measured with the membrane) relates to the intrinsic contact angle $\theta_{w,0}$ (i.e., the water contact angle measured with a molecularly smooth, nonporous surface made of the same material as the membrane) via the following equation.[155]

$$\cos \theta_{w,A} = \phi(\cos \theta_{w,0} + 1) - 1 \quad (12)$$

The simplest and most common fabrication technique to create a superhydrophobic membrane is to coat the membrane surface with nanoparticles grafted with perfluorinated or other ultralow surface energy,[95,96] although many other techniques can also be used.[96,112] In all cases, the major requirement is that the membrane surface has a high degree of roughness and low surface energy.

Several studies have shown that scaling can be mitigated with superhydrophobic membranes to different extents depending on the scaling type and other factors.[95,96,112,113,156] With the use of superhydrophobic membranes, gypsum scaling was substantially delayed, and NaCl scaling was not even observed.[96,112,113] Also, the superhydrophobic membrane also showed promising effectiveness in reducing mineral scaling in MD treatment of industrial wastewater such as the blowdown water from the cooling tower of a power plant.[95] Although the exact mechanisms of scaling mitigation by superhydrophobic membranes are unclear, there are several possible explanations. First, the small liquid–solid contact area with a superhydrophobic membrane reduces the area available for crystal deposition or nucleation on the membrane surface (Figure 7A). For example, consider a hydrophobic and superhydrophobic membrane made from the same material with $\theta_{w,0} = 105°$. For the rough, superhydrophobic membrane with $\theta_{w,A} = 165°$, the areal fraction of liquid–solid contact ϕ is estimated to be only ~5% based on eq 7. In comparison, for the hydrophobic membrane with $\theta_{w,A} = 120°$, ϕ is estimated to be ~67%. The larger liquid–solid contact offers more area for heterogeneous nucleation and crystal deposition and/or adhesion (Figure 7B).

https://dx.doi.org/10.1021/acsestengg.0c00025
ACS EST Engg. 2021, 1, 117–140

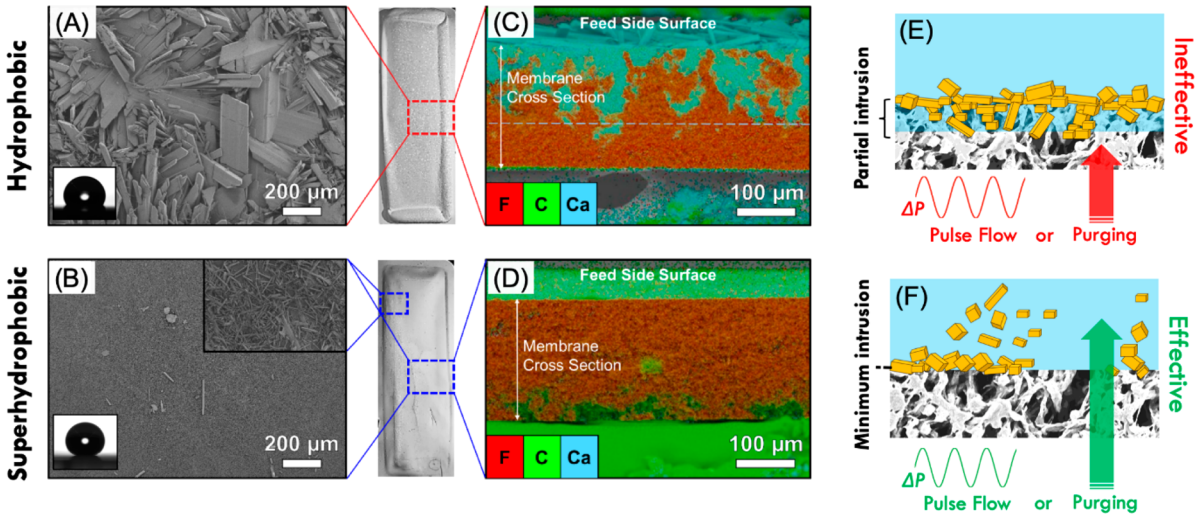

Figure 8. (A) Top-down SEM image and (B) cross-section elemental mapping based on SEM with EDS for a hydrophobic membrane scaled with gypsum. (C) Top-down SEM image and (D) cross-section elemental mapping based on SEM-EDS for a superhydrophobic membrane. In both cases, the membranes were subject to intermittent back-purging of the same frequency, duration, and intensity. (E, F) Illustration of how (E) partial pore intrusion into hydrophobic membrane or (F) the lack of it with superhydrophobic membrane influences the effectiveness of scaling mitigation by purging or pulse flow. Adapted with permission from ref 174.

The second possible explanation of the scaling mitigation by a superhydrophobic membrane is the reduced propensity for heterogeneous nucleation, which can be explained by the CNT and eq 7 introduced in the last section. Equation 7 suggests that the nucleation on an interface with higher $\theta_{n/w}$ is more difficult, because $f(\theta_{n/w})$ is a monotonically increasing function for $\theta_{n/w} \in [0,\pi]$. As discussed earlier, $\theta_{n/w}$ positively correlates with the intrinsic (in-air) water contact angle $\theta_{w,A}$. Therefore, we should expect that nucleation on a surface with lower surface energy γ_s also has a higher energy barrier than nucleation on a surface with higher γ_s. Consequently, nucleation propensity is substantially lower with a superhydrophobic membrane for two reasons. First and most importantly, with a superhydrophobic membrane, there is a larger fraction of the liquid−air interface (Figure 7C), which has the lowest nucleation propensity (as $\gamma_s \approx 0$ for air). Second, because the fabrication of a superhydrophobic membrane typically uses materials (e.g., perfluorinated compounds) with a lower γ_s than that used for fabricating hydrophobic membranes (e.g., poly(vinyl difluoride) or polypropylene), the nucleation propensity on the liquid−solid interface is also lower with a superhydrophobic membrane (Figure 7C) than with a hydrophobic membrane (Figure 7D).

The third explanation of scaling mitigation by a superhydrophobic membrane is the slip boundary condition for liquid flow along the membrane surface (Figure 7E). The slip boundary condition may have two major impacts on scale formation.[113] The first impact is the reduced residence time for crystal growth and interaction with a superhydrophobic membrane surface as compared to that for a flow along a hydrophobic membrane with a no-slip condition (Figure 7F). The second impact is the higher flow velocity and turbulence intensification near the surface of a superhydrophobic membrane. This second effect may reduce the oversaturation level near the membrane surface by promoting better mixing to minimize the concentration polarization. It may also aid in dislodging precipitated crystals or even preventing their deposition.[117]

The first and second explanations of scaling mitigation concern the free energy of a system, which is essentially a thermodynamic argument. In comparison, the third contribution is a hydrodynamic argument. While all these explanations are mechanistically reasonable, to what extent each explanation contributes to the overall effect of scaling mitigation by superhydrophobic membrane is practically difficult to quantify.

Operation Strategies. Besides pretreatment and the use of superhydrophobic membranes, various operation strategies can also reduce mineral scaling in MD. These strategies include water flushing,[133] microbubble aeration,[157] electrophoretic mixing,[158] flow/temperature reversal,[159] and MD integrated with a crystallizer,[116,160−167] which hinder scaling by either removing scalants from the feedwater or disrupting the nucleation process. For example, periodic flushing using deionized water has been shown to maintain a stable water vapor flux of MD in gypsum-saturated feed solutions, probably due to the removal of gypsum nuclei from the membrane surface.[133] However, the use of deionized water (product of MD) for cleaning is not desirable, and the effectiveness of this approach diminishes as more water is recovered. In another study, flow and temperature reversal between feed and distillate streams was proved effective in mitigating mineral scaling when using MD to treat hypersaline water from the Great Salt Lake.[159] Furthermore, microbubbles have been also used to effectively reduce vapor flux decline caused by salt precipitation. The authors proposed that the negatively charged microbubbles not only reduced the effect of concentration polarization but also attracted divalent ions (e.g., Ca^{2+} and Mg^{2+}) at the water−air interface to reduce their availability in the bulk solution for scale formation.[157] Scaling mitigation can also be achieved by applying an alternating current to the surface of electrically conducting membranes fabricated via depositing a network of carbon nanotubes on a hydrophobic membrane.[158] Such a strategy has been shown to be effective for mitigating both gypsum and silica scaling, likely due to the electrophoretic mixing that disrupts the concentration polarization layer. Also, the generation of an electrical double layer creates a concentration imbalance

https://dx.doi.org/10.1021/acsestengg.0c00025
ACS EST Engg. 2021, 1, 117−140

between anions and cations, which also contributes to slowing the scale formation.[158]

Another integrated process that has the benefit of pure water recovery while simultaneously recovering valuable precipitates is membrane distillation-crystallization (MDC). In MDC, MD is used to concentrate the aqueous solution to the desired supersaturation, while a crystallizer is used to precipitate and remove mineral crystals from the solution. While the integration of MD with a brine crystallizer may allow for an enhanced water recovery ratio and delay scaling induction time,[168,169] the MD membrane is still subjected to high saturation solutions and, thus, eventually suffers from mineral scaling.[170,171]

Backwashing is a common strategy for membrane cleaning in microfiltration.[172,173] Because an MD membrane needs to be maintained nonwetted, back-purging (with gas) can be used instead of backwashing (with water). It has been found that intermittently back-purging a hydrophobic membrane cannot mitigate gypsum scaling due to the robust adhesion of the scale layer to the hydrophobic membrane surface (Figure 8A). However, when intermittent back-purging is combined with superhydrophobic membranes, gypsum scaling can be virtually eliminated (Figure 8 B), even though the use of a superhydrophobic membrane alone without back-purging can only delay gypsum scaling.[174] Back-purging a hydrophobic membrane was ineffective, because the partial intrusion of the feedwater into the pores promotes very robust adhesion of the formed crystal to the membrane (Figure 8C,E). In comparison, the minimum solid−liquid contact area and lack of pore intrusion in the case of a superhydrophobic membrane makes back-purging effective (Figure 8D,F).

In a more recent study, a similar approach integrating superhydrophobic membrane and pulse flow (i.e., flow with a variable hydraulic pressure) was shown to be also effective in eliminating gypsum scaling.[175] Again, neither pulse flow with hydrophobic membrane nor superhydrophobic membrane alone without pulse flow was effective in mitigating gypsum scaling. While pulse flow is likely more practical than back-purging in a real operation, both studies reveal that the same importance of synergy between the material and operation strategies in mitigating gypsum scaling. Regardless of the specific operation approach, recharging the air layer on the surface of a superhydrophobic membrane seems to be critical to sustain long-term MD performance against gypsum scaling. Other approaches toward this goal of air-layer recharging, including the direct injection of nanobubbles or the in situ generation of bubbles via electrolysis, may be explored. Finally, it is not entirely clear why a superhydrophobic membrane alone, without back-purging or pulse flow, can effectively eliminate scaling by NaCl but not gypsum. We can only postulate at this point that the crystal morphology plays an important role. Elucidating the impact of scaling type on the effectiveness of different scaling mitigation approaches is important for developing strategies that are universally effective for real feedwater with complex compositions.

FOULING

Fouling is a common problem to all membrane processes and is an umbrella term that can include organic fouling, inorganic fouling, and biological fouling. In MD processes, mineral scaling has been referred to as inorganic fouling in some cases. However, inorganic fouling in other membrane processes often involves only inorganic particles that originally exist in the feedwater, excluding mineral scaling. This type of inorganic fouling (sometimes referred to as colloidal fouling) is not a major concern in MD or MC, as inorganic particles can be readily removed using simple pretreatments. Therefore, we will focus on organic and biological fouling in this discussion.

Generally speaking, fouling is a membrane failure common in both MD and MD applications, where species in the feed solution accumulate on the membrane surface and block its pores, reducing the flux of water vapor (in MD) and volatile component (in MC), and it may eventually lead to pore wetting.[124,176] From an operational perspective, the low operating pressure in MC and MD reduces the propensity to form a dense, compact, irreversible foulant layer as compared to pressure-driven membrane processes such as RO or NF.[177,178] From a material perspective, however, MD and MC membranes are inherently prone to organic fouling due to the long-range hydrophobic interaction between the hydrophobic membrane and many common hydrophobic organic foulants.[179,180]

The most common method for detecting membrane fouling is by simply monitoring the flux of water vapor (in MD) or volatile species (in MC), which declines as the membrane becomes fouled. Several studies have also used electro-impedance spectroscopy to detect organic fouling in situ.[181−184] In brief, the working mechanism is that the foulant layer adds electrical resistance to the membrane surface. This new detection technique allows for the elucidation of the mechanisms and time scales of organic fouling, which in turn enables early fouling detection, more efficient operation, and more effective fouling mitigation in practice.

Organic foulants relevant to MD and MC include proteins, humic acids, and, in some cases, emulsified oil droplets. Oil fouling is relevant to MD, because MD has been actively explored for treating oil- and gas-produced water.[4,73,152] Biological fouling (or just biofouling) is caused by the growth of bacteria, fungi, and algae, especially by the formation of biofilm. Technically, organic foulants are also found in biofouling, as substances from microbes, including proteins and extracellular polymeric substances, are organics. In this section we will review the mechanisms in which these foulants interact with the membrane surfaces, making the distinction between the saline conditions typical to MD and lack thereof in MC. In particular, we will discuss the effects of solution composition on fouling mechanisms and how these mechanisms apply to each of the individual foulant categories. Finally, we will review the common, and most effective, mitigation strategies that have shown promise for practical MC and MD applications.

Mechanism of Organic Fouling. In general, organic fouling is a phenomenon where organic colloids interact with a membrane surface in an attractive manner and accumulate to cover the membrane surface. Colloidal interaction is often modeled by the Derjaguin−Landau−Verwey−Overbeek (DLVO) theory, which considers the relative contributions of the electric double layer (EDL) and van der Waals (vdW) interactions. The EDL interaction, which is repulsive for two similarly charged interacting surfaces, is strongly dependent on the ionic strength. In the context of MD, which is most promising for desalinating hypersaline brine, the ionic strength is so high that no interaction energy barrier should exist, because the vdW contribution always outcompetes the EDL contribution. Therefore, it may be argued that the DLVO theory is less relevant to MD due to the lack of interaction

https://dx.doi.org/10.1021/acsestengg.0c00025
ACS EST Engg. 2021, 1, 117−140

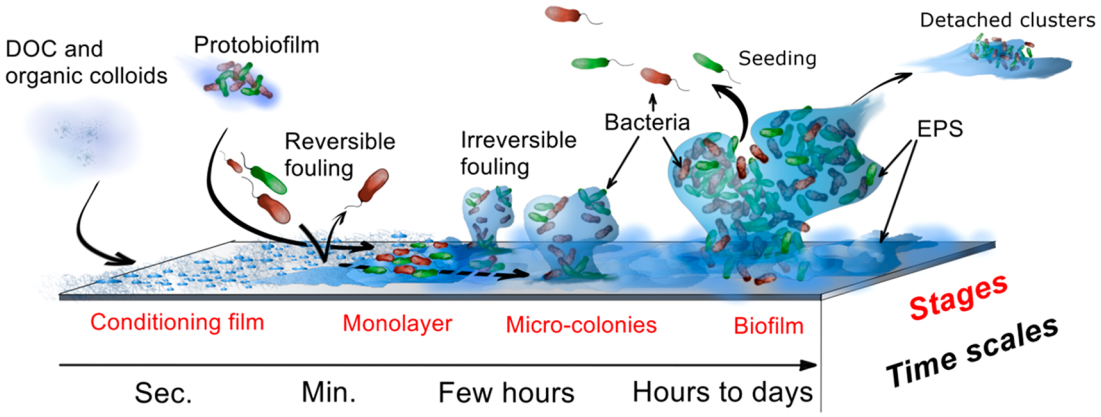

Figure 9. Different stages of biofilm formation and the respective time scales. Dissolved and colloidal organics deposit onto the surface and form a conditioning film to which bacteria adhere. Protobiofilm and bacteria then directly deposit onto the conditioning film. These two processes occur on the time scale of minutes to seconds, but eventually the EPS excreted from the bacteria enhances the cell attachment and facilitates the formation of a robust and continuous biofilm. The biofilm eventually becomes a source from which bacteria and bacterial clusters are dispersed. Adapted with permission from ref 196.

energy barrier in any practical condition. The DLVO theory may be relevant to understanding fouling propensity in the context of MC, where salinity (and thus ionic strength) can be quite low. Even so, the DLVO theory should only be used to provide qualitative reasoning for the observed phenomena but should not be used as a predictive tool to quantify the fouling propensity. Specifically, a microporous hydrophobic membrane is different in many aspects from the idealized impermeable surface in a particle deposition to which the DLVO theory has been applied.

Another important interaction that is strongly relevant to the organic fouling of hydrophobic membranes is the long-ranged, hydrophobic interaction.[179,180,185] The hydrophobic interaction is associated with the configurational rearrangement of water molecules and tends to be an order of magnitude stronger and longer-ranged than the vDW interactions, decaying exponentially with distance.[179] The exact mechanism of the widely observed hydrophobic interaction has long been debated. One probable explanation is the capillary bridging between two surfaces by an air bubble that tend to develop on a hydrophobic surface.[186,187] With this mechanism, a hydrophobic interaction is all the more relevant to MD and MC, not only because hydrophobic membranes are used but also because an air layer is intrinsically present in a nonwetted membrane in a Cassie−Baxter state. Considering the substantially high strength of the hydrophobic interaction and the heavily shielded EDL interaction in high ionic strength, we argue that the long-ranged hydrophobic interaction dominates the membrane fouling process, making hydrophobic organic foulants very troublesome for sustaining long-term MD or MC performance.[188,189] This is particularly true for oil foulants that are not heavily emulsified by excessive surfactants.

Mechanism of Biofouling. Biofouling pertains to both MC and MD when feedwater containing a high content of biological microorganisms, such as those in the wastewaters of the pharmaceutical, food and beverage industries, and municipal wastewater treatment facilities, is in direct contact with the membrane surface.[27,190] The high-salinity and high-temperature conditions of the feed solution in MD may lead one to expect a low potential for biofouling.[191] However, there are bacteria and other microorganisms that are resistant to high salinity and temperature,[192] and moderate temperature can even promote the growth of thermophilic bacteria.[176,193,194] While the mechanism of biofouling is complicated due to the presence of multiple foulant species with different physico-chemical properties, it is important to discuss the general process and time scales of biofouling.

Biofouling is a particularly unwelcome fouling phenomenon, because it would lead to the formation of a large gel-like structure on the membrane surface. Such a structure, namely "biofilm," is difficult to remove physically or via chemical cleaning.[195] The growth of biofilm is typically characterized by several unique stages that develop consecutively[195] (Figure 9). In the early stages of biofouling, a conditioning film develops, where organic foulants such as proteins, humic substances, and other organic matter deposit on the membrane surface in a film with thickness on the order of nanometers.[195,196] The conditioning film from organic fouling serves as a precursor for further foulants attachment, as it alters the surface properties exposed to the feed solution.[197−200] Next, several attractive interactions, including vdW, hydrophobic, and hydrogen-bonding interactions, result in reversible bacteria cell attachment, while larger aggregate particles and protein aggregates (namely, "protobiofilms") irreversibly attach to the conditioning film.[197] These two processes occur on the time scale of seconds to minutes. After a few hours, the bacteria cells bind irreversibly to the surface. This irreversible attachment is due to the reinforcement of the extracellular polymeric substances (EPS), which are produced within the microbe colonies of the biofilm and mostly consist of protein, polysaccharides, some humic substances, and DNA.[176,193,195,201]

The kinetic growth and mechanical properties of the EPS are heavily influenced by the salinity and specific ionic species.[202] For example, the presence of divalent cations such as calcium and magnesium is known to reinforce the biofilm by forming complexes with the polysaccharides in the EPS matrix, forming a more dense, interconnected network.[195,201,203] Furthermore, divalent cations in the feedwater aid the initial adhesion of organic foulants, such as humic substances, by forming complexes in the bulk that settle more easily and deposit on the membrane surface.[134,204−206] After several hours up to days, the biofilm is fully reinforced by the constant secretion of

https://dx.doi.org/10.1021/acsestengg.0c00025
ACS EST Engg. 2021, 1, 117−140

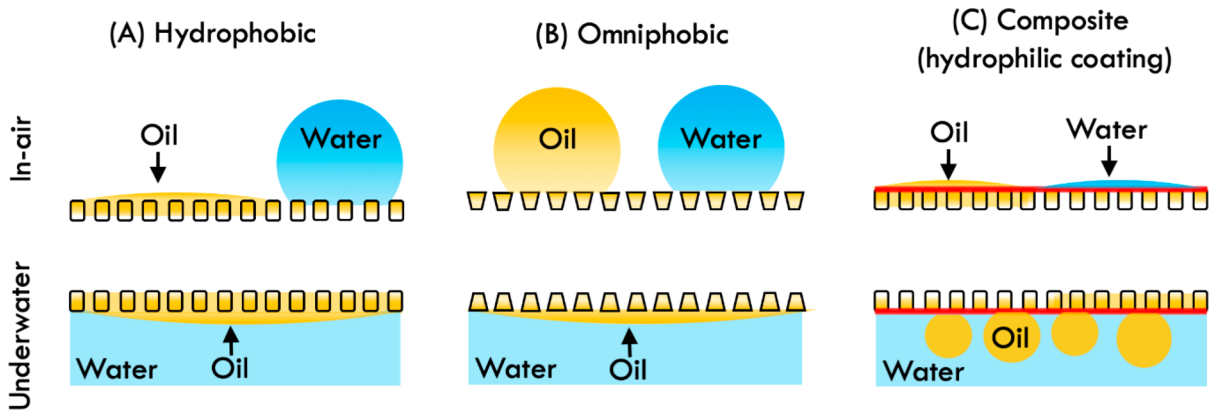

Figure 10. Comparison between in-air (top) and underwater (bottom) wetting properties for (A) hydrophobic membrane, (B) omniphobic membrane, and (C) composite membrane with a hydrophobic substrate and a hydrophilic coating.

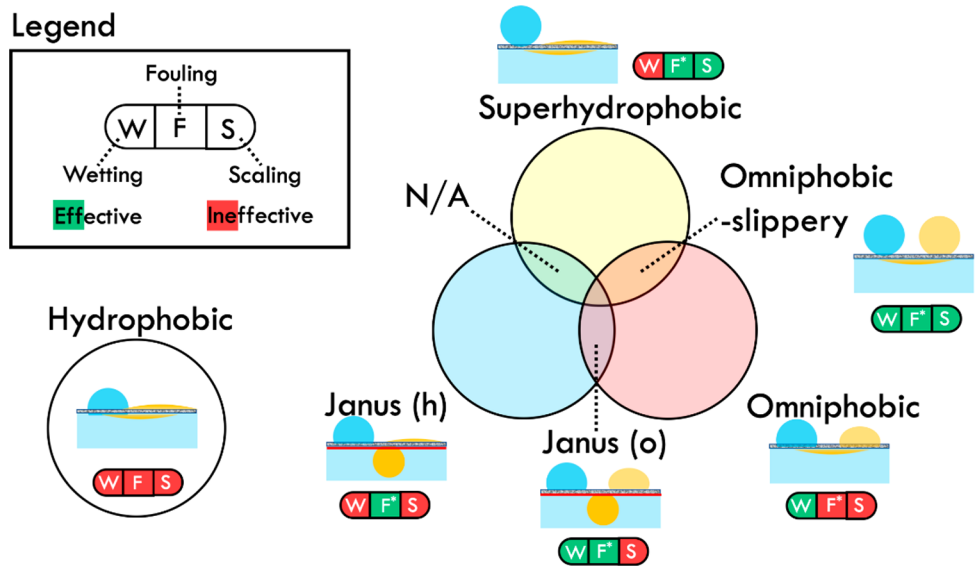

Figure 11. Illustration of the effectiveness of different types of membranes with special wetting properties in mitigating wetting, fouling, and scaling. A Janus (h) membrane is a membrane with a hydrophobic (thus "h") substrate and an in-air hydrophilic and underwater oleophobic coating (denoted by the red line in the figure). A Janus (o) membrane is a membrane with an omniphobic (thus "o") substrate and an in-air hydrophilic and underwater oleophobic coating. An omniphobic-slippery membrane is both omniphobic and superhydrophobic (i.e., slippery). The superscript "*" for "F" (representing fouling) indicates the uncertainty or limited information for the effectiveness evaluation, primarily because of the multiple types of fouling that have not been comprehensively assessed for the respective membranes. These effectiveness ratings are based on the following studies: superhydrophobic membranes,[95,96,112,113,153,154,174] omniphobic membranes,[28,73−82] Janus (h) membranes,[38,188,189,219,220,235−237] Janus (o) membranes,[219,238] and omniphobic-slippery membranes.[239]

EPS and can even begin to spread and grow with the colonization of new areas on the membrane by living bacteria from within the biofilm.[195]

Fouling Mitigation Strategies. *Pretreatments and Membrane Cleaning.* Well-established physical and chemical pretreatments can be used to reduce the concentration of foulants in the feed solution. Physical pretreatments are often very effective in mitigating membrane fouling. For example, pretreatment with nanofiltration or ultrafiltration very effectively limits flux decline due to fouling.[33,36,42] Coagulation/flocculation is a highly cost-effective approach to remove foulants from the feed solution by forming flocs that enmesh the foulants. These flocs can be removed by sedimentation, filtration through porous media, or microfiltration.[5,151,207] For example, coagulation pretreatment of recirculating cooling water with poly(aluminum chloride) has shown to improve elimination of total organic carbon and reduce the water vapor flux decline due to organic fouling in MD.[151] Other methods that may also be effective include flotation (especially for oil foulants) and activated carbon adsorption. A recent study using MD to treat real produced water from the shale oil and gas industry showed that precipitative softening/coagulation using aluminum sulfate followed by walnut shell filtration can very effectively reduce fouling in MD.[152] We expect that pretreatment methods or treatment trains that have been proven effective for fouling mitigation in other membrane processes are also effective for MD and that the choice of pretreatments for fouling mitigation depends largely on the feedwater characteristics rather than the membrane processes.

In addition to pretreatment, there are additional chemical and physical strategies that are effective in removing foulants that have already attached to membrane surfaces. For example, the use of micro/nanobubbles via direct injection into the feed

https://dx.doi.org/10.1021/acsestengg.0c00025
ACS EST Engg. 2021, 1, 117−140

solution[157,208−211] or using ultrasound or electrolysis to induce bubble nucleation near the membrane surface[212−215] has been shown to effectively limit and remove organic foulants. Generally speaking, the bubbles both physically dislodge foulants from the membrane surface and remove foulants from the feedwater by capturing them at the air−liquid interface of the bubbles (similar to flotation).[215−217] In a study where membrane biofouling occurred in the MD desalination of seawater from the South China Sea, ultrasonic cleaning effectively removed the organic foulants, and transmembrane water vapor flux was restored to its initial rate.[213] Other common membrane cleaning methods, including those using cleaning agents based on alkaline, acidic, surfactant, and chelating agents, have also been shown to be effective to different extents for removing the foulant layer.[23,218]

While pretreatment methods that are effective for organic fouling mitigation can also reduce biofouling to a certain degree via reducing the microbe concentration of the feed solution, methods for cleaning organic fouling may not be effective for alleviating biofouling, especially after biofilms have formed on the membrane surface. The most effective approach for preventing biofouling or cleaning a biofilm once it forms is to apply disinfectants (e.g., chlorination).[178] Because most disinfectants are also strong oxidants, disinfection is not applicable for RO or NF membranes that are primarily based on a polyamide that would suffer a performance loss after prolonged exposure to oxidants.[178] For MD, however, applying disinfectants can be a viable approach, because hydrophobic membranes, especially those made from fluoropolymers, are typically chemically stable.

Fouling-Resistant Membranes. Many recent studies on MD fouling are focused on oil fouling, because it presents a critical challenge when MD is used to desalinate oil- and gas-produced water. Hydrophobic MD membranes are inherently prone to oil fouling due to the strong hydrophobic interaction. Oil fouling is fatal to a hydrophobic membrane, because it is difficult to be reversed due to pore wicking by oil (Figure 10A). It may be expected that an omniphobic membrane is resistant to oil fouling, because an omniphobic surface is, by definition, both hydrophobic and oleophobic. However, it is important to emphasize that all wetting properties, without a prefix descriptor, are defined in air. An omniphobic surface (and membrane) is in-air oleophobic but not underwater oleophobic. In fact, an omniphobic membrane is underwater oleophilic,[38] because the low surface energy of the material required for fabricating an omniphobic membrane leads to a strong hydrophobic interaction just as that between oil droplets and a hydrophobic membrane. However, an omniphobic membrane differs from a hydrophobic membrane by having a reentrant structure that prevents the oil droplets from wicking into the pores (Figure 11B). In other words, while oil droplets can still foul an omniphobic membrane by covering the membrane surface and blocking pores for vapor transfer, the fouling can be reversed by cleaning due to the absence of pore wicking. Interestingly, if the oil-in-water emulsion is stabilized by a high concentration of surfactants, an omniphobic membrane would not even be fouled, because now both the oil droplets and the membrane surface are rendered hydrophilic due to the adsorbed surfactants, thereby eliminating the attractive hydrophobic interaction.[38] While the same principle should apply to hydrophobic membranes, hydrophobic membranes are susceptible to wetting by surfactants.

On the basis of underwater wettability, a robust material strategy to develop an MD or MC membrane resistant to oil fouling is to apply a (in-air) hydrophilic coating layer on a hydrophobic membrane surface[38,188,189,219,220] (Figure 10C). An in-air hydrophilic surface is typically underwater oleophobic due to the hydration layer that results from the strong attractive interaction between water and the high surface energy moieties of the hydrophilic coating. This hydration layer prevents oil fouling, as the spreading of oil on the membrane surface requires dehydration of the coating layer, which is energetically unfavorable.[189] The mitigation of fouling using such a hydration layer is more robust, as the "nonfouling" condition is a thermodynamically stable state.

Finally, we note that in-air hydrophilicity is only a necessary, but not a sufficient, condition for underwater oleophobicity. To develop a robust underwater oleophobic surface, the effects of electrostatic interaction between oil and surface must also be considered. For example, while a negatively charged (in-air) hydrophilic surface is robustly resistant to fouling by negatively charged oil droplets,[221,222] a positively charged (in-air) hydrophilic surface has shown to be underwater oleophobic only upon its initial contact with a solution containing negatively charged oil droplets. Over the time scale of tens of minutes, the positively charged (in-air) hydrophilic becomes increasingly oleophilic and wetted by the oil droplets of opposite charge.[221] Expectedly, the MD membrane with a negatively charged hydrophilic coating is substantially more robust in sustaining a stable MD performance than that with a positively charged hydrophilic coating, because the former is robustly underwater oleophobic, while the latter is not. Ultimately, it is the underwater wetting property that matters for oil-fouling resistance.

In general, this rationale also applies to the mitigation of organic foulants other than oil droplets, such as NOM and proteins. Hydrophilic surfaces with identical charge to the organic foulants in question are more robust in mitigating fouling due to the presence of a hydration layer and electrostatic repulsion.[223−231] This is especially true for organic foulants with hydrophobic moieties such as proteins. Somewhat paradoxical to the observation that an in-air hydrophilic, underwater oleophobic surface imparts robust fouling resistance, some studies have also reported that superhydrophobic membranes are also effective for mitigating fouling by organics such as humic substances.[232−234] Similar to the mechanisms for scaling mitigation, mitigating organic fouling with a superhydrophobic membrane is more attributable to decreased liquid−solid contact between the feed solution and membrane surface. Because there is still some small fraction of liquid−solid contact, long-term biofouling experiments show a small flux decline, as the humic substances eventually attach to the surface where there is that liquid−solid contact.[232,233]

■ OUTLOOK

Despite the several unique advantages of MD in desalinating hypersaline brine, MD also faces multiple unique challenges as compared to pressure-driven membrane processes that have been scaled up for practical applications. For example, virtually all "sweet spot" applications for MD involve concentrating high-salinity streams, which inherently has a higher propensity for mineral scaling than other membrane processes treating feedwater with low to moderate salinity.[1,6] Furthermore, pore wetting is a technical challenge that is relevant to MD (or MC) but not to any other membrane processes. Lastly, while fouling

https://dx.doi.org/10.1021/acsestengg.0c00025
ACS EST Engg. 2021, 1, 117−140

is common in all membrane processes, the use of a hydrophobic membrane and the presence of an air layer in MD processes enhances the hydrophobic interaction and, thereby, increases the propensity of fouling by hydrophobic organics.[189] Nonetheless, the absence of an applied hydraulic pressure in MD prevents the formation of a very dense foulant layer, which may alleviate irreversible fouling.[177,178] Any of these three problems, scaling, wetting, and fouling, if not properly addressed, can substantially compromise the performance or even lead to a complete process failure of MD (or MC).

Fortunately, the rich collective experience in other membrane processes can help us address the problems of fouling and scaling using the proper measures of pretreatment, feedwater conditioning, (e.g., dosing antiscalants or disinfectants), and membrane cleaning. These approaches, though not scientifically novel, are often economical and effective over a broad range of foulants or scalants. Other process innovations, such as the use of micro/nanobubbles, intermittent backpurging, and pulse flow, have also been proven effective in enhancing the robustness of the MD performance.[157,174,175] However, these approaches have their limitations. For example, the challenge of pore wetting is difficult to overcome by removing wetting agents from the feedwater due to the very limited capability of achieving such a separation cost-effectively. In this case, developing novel MD membranes with special wettability provides an alternative path for addressing the challenge of pore wetting. For fouling and scaling, developing better membranes is also an important supplement to, or even a substitute of, pretreatments and operational measures. In certain cases, the material and operational approaches are synergistic and do not function effectively without each other.

Thanks to the recent development of novel membranes with special wetting properties, we now have effective solutions to each of the three major challenges in MD: wetting, scaling, and fouling. The general rules of thumb are that (1) omniphobic membranes can prevent wetting, (2) superhydrophobic membranes are effective in mitigating mineral scaling, and (3) Janus membranes (i.e., composite membranes) with an in-air hydrophilic and underwater oleophobic coating are capable of reducing fouling, in particular, oil fouling. However, none of these membranes have been proven to be a robust and universal solution to all three challenges. To engineer resistance against multiple failure mechanisms, it is possible to integrate two types of wetting properties into one composite membrane. For example, a Janus (o) membrane, which comprises an omniphobic substrate and a fouling-resistant, hydrophilic surface coating, has been shown to be effective in mitigating both wetting and fouling.[219] In another example, a membrane that is both omniphobic and superhydrophobic (also known as slippery) has been shown to be simultaneously wetting and scaling resistant.[239] These general principles are summarized in Figure 11.

The effectiveness of different membranes in mitigating organic and biological fouling is less clear-cut, as different types of foulants behave very differently, and not all types of fouling (e.g., oil, natural organic matter, and biological foulants) have been tested with membranes with different types of wetting properties. Membranes that are resistant to fouling by natural organic matter may not be resistant to oil fouling, and vice versa. Moreover, even the oil-fouling resistance of the same membrane also depends on whether and to what extent the oil droplets are stabilized by surfactants. When oil droplets are stabilized by excessive surfactants, the membrane may fail via the mechanism of wetting instead of fouling.[38]

In some cases, all types of failure mechanisms in MD have been referred to as "fouling". For example, a membrane might be referred to as "anti-fouling", while it was actually tested against a variety of agents that would induce wetting, scaling, and fouling (of the narrower definition).[9,36,240] While putting all these mechanisms under the umbrella of fouling may sound pragmatically convenient from an operation point of view (it essentially becomes a proxy term for "membrane failure"), doing so obscures the fundamental difference behind these mechanisms and is unconstructive for the systematic understanding of membrane failure and the development of mitigation strategies. In other cases, however, the membrane fails via multiple mechanisms concurrently, and distinction between them is inherently difficult, because one type of failure can induce the other. For example, it has been reported that both organic fouling and mineral scaling can result in pore wetting.[37] In the case of gypsum scaling, wetting is caused by pore deformation instead of the reduced surface tension of the feed solution due to the presence of surfactants or LST liquids.[35]

In addition to more clearly distinguishing between different failure mechanisms, we also need to be more mindful and precise in categorizing a membrane with special wettability. For instance, a superhydrophobic membrane can be both oleophobic and oleophilic. When a study shows that a superhydrophobic membrane is wetting resistant without actually measuring the oil-wetting property of the membrane, the conclusion can be confusing—the wetting resistance may likely be attributable to the oleophobicity imparted by the re-entrant structure instead of the superhydrophobicity imparted by the high degree of roughness.

Finally, although a limited number of MD studies was performed using real feedwater such as RO brines or industrial wastewater, a majority of reported studies on addressing the challenges of wetting, scaling, and fouling in MD, especially those related to novel membrane development, used simple feed solutions. Most studies either focused on a single type of membrane failure or investigated multiple mechanisms separately. While these studies are important to enhancing our fundamental understanding, practical MD processes often involve more complex feed solutions and the synergy of different failure mechanisms. Examples include, but are not limited to, scaling by different types of minerals, simultaneous mineral scaling and organic fouling, and simultaneous fouling and wetting. Therefore, future research efforts on pretreatment, operation, or membrane development should be more directed toward understanding the combined effects of multiple failure mechanisms using feed solutions with more complex compositions. Such efforts will potentially bridge the gap between fundamental understanding and engineering practice, thereby enabling MD to become a reliable process for treating various types of hypersaline brine.

AUTHOR INFORMATION

Corresponding Authors

Tiezheng Tong − *Department of Civil and Environmental Engineering, Colorado State University, Fort Collins, Colorado 80523, United States;* orcid.org/0000-0002-9289-3330; Email: tiezheng.tong@colostate.edu

https://dx.doi.org/10.1021/acsestengg.0c00025
ACS EST Engg. 2021, 1, 117−140

Shihong Lin − *Department of Chemical and Biomolecular Engineering and Department of Civil and Environmental Engineering, Vanderbilt University, Nashville, Tennessee 37235-1831, United States;* orcid.org/0000-0001-9832-9127; Email: shihong.lin@vanderbilt.edu

Authors

Thomas Horseman − *Department of Chemical and Biomolecular Engineering, Vanderbilt University, Nashville, Tennessee 37235-1831, United States;* orcid.org/0000-0002-4660-1448

Yiming Yin − *Department of Civil and Environmental Engineering, Colorado State University, Fort Collins, Colorado 80523, United States*

Kofi SS Christie − *Department of Civil and Environmental Engineering, Vanderbilt University, Nashville, Tennessee 37235-1831, United States;* orcid.org/0000-0002-7039-7889

Zhangxin Wang − *Department of Chemical and Environmental Engineering, Yale University, New Haven, Connecticut 06511, United States*

Complete contact information is available at: https://pubs.acs.org/10.1021/acsestengg.0c00025

Notes

The authors declare no competing financial interest.

■ ACKNOWLEDGMENTS

The authors are grateful for the generous support by the National Science Foundation via Grant Nos. 1739884 (S.L.), 1705048 (T.H. and Z.W.), and DGE-1145194 (K.S.S.C.) and by the Bureau of Reclamation (USBR) under the Department of Interior via DWPR Agreement R18AC00108 (T.T.).

■ REFERENCES

(1) Deshmukh, A.; Boo, C.; Karanikola, V.; Lin, S.; Straub, A. P.; Tong, T.; Warsinger, D. M.; Elimelech, M. Membrane Distillation at the Water-Energy Nexus: Limits, Opportunities, and Challenges. *Energy Environ. Sci.* **2018**, *11* (5), 1177−1196.
(2) Lawson, K. W.; Lloyd, D. R. Membrane Distillation. *J. Membr. Sci.* **1997**, *124* (1), 1−25.
(3) Alkhudhiri, A.; Darwish, N.; Hilal, N. Membrane Distillation: A Comprehensive Review. *Desalination* **2012**, *287*, 2−18.
(4) Shaffer, D. L.; Arias Chavez, L. H.; Ben-Sasson, M.; Romero-Vargas Castrillón, S.; Yip, N. Y.; Elimelech, M. Desalination and Reuse of High-Salinity Shale Gas Produced Water: Drivers, Technologies, and Future Directions. *Environ. Sci. Technol.* **2013**, *47* (17), 9569−9583.
(5) Sardari, K.; Fyfe, P.; Lincicome, D.; Ranil Wickramasinghe, S. Combined Electrocoagulation and Membrane Distillation for Treating High Salinity Produced Waters. *J. Membr. Sci.* **2018**, *564*, 82−96.
(6) Tong, T.; Elimelech, M. The Global Rise of Zero Liquid Discharge for Wastewater Management: Drivers, Technologies, and Future Directions. *Environ. Sci. Technol.* **2016**, *50* (13), 6846−6855.
(7) Choi, Y.; Naidu, G.; Nghiem, L. D.; Lee, S.; Vigneswaran, S. Membrane Distillation Crystallization for Brine Mining and Zero Liquid Discharge: Opportunities, Challenges, and Recent Progress. *Environ. Sci. Water Res. Technol.* **2019**, *5* (7), 1202−1221.
(8) Lin, S. Energy Efficiency of Desalination: Fundamental Insights from Intuitive Interpretation. *Environ. Sci. Technol.* **2019**, *54* (1), 76−84.
(9) Tijing, L. D.; Woo, Y. C.; Choi, J. S.; Lee, S.; Kim, S. H.; Shon, H. K. Fouling and Its Control in Membrane Distillation-A Review. *J. Membr. Sci.* **2015**, *475*, 215−244.
(10) Christie, K. S. S.; Horseman, T.; Lin, S. Energy Efficiency of Membrane Distillation: Simplified Analysis, Heat Recovery, and the Use of Waste-Heat. *Environ. Int.* **2020**, *138*, 105588.
(11) Lin, S.; Yip, N. Y.; Elimelech, M. Direct Contact Membrane Distillation with Heat Recovery: Thermodynamic Insights from Module Scale Modeling. *J. Membr. Sci.* **2014**, *453*, 498−515.
(12) Camacho, L. M.; Dumée, L.; Zhang, J.; Li, J. De; Duke, M.; Gomez, J.; Gray, S. Advances in Membrane Distillation for Water Desalination and Purification Applications. *Water* **2013**, *5* (1), 94−196.
(13) Gingerich, D. B.; Mauter, M. S. Quantity, Quality, and Availability of Waste Heat from United States Thermal Power Generation. *Environ. Sci. Technol.* **2015**, *49* (14), 8297−8306.
(14) Burgess, G.; Lovegrove, K. Solar Thermal Powered Desalination: Membrane Versus Distillation Technologies*Solar* **2005**.
(15) Qiblawey, H. M.; Banat, F. Solar Thermal Desalination Technologies. *Desalination* **2008**, *220*, 633−644.
(16) Wang, Z.; Horseman, T.; Straub, A. P.; Yip, N. Y.; Li, D.; Elimelech, M.; Lin, S. Pathways and Challenges for Efficient Solar-Thermal Desalination. *Sci. Adv.* **2019**, *5* (7). .
(17) Curcio, E.; Drioli, E. Membrane Distillation and Related Operations - A Review. *Sep. Purif. Rev.* **2005**, *34* (1), 35−86.
(18) Rongwong, W.; Lee, J.; Goh, K.; Karahan, H. E.; Bae, T.-H. Membrane-Based Technologies for Post-Treatment of Anaerobic Effluents*npj Clean Water***2018***11* DOI: 10.1038/s41545-018-0021-y
(19) Yu, X.; An, L.; Yang, J.; Tu, S. T.; Yan, J. CO2 Capture Using a Superhydrophobic Ceramic Membrane Contactor. *J. Membr. Sci.* **2015**, *496*, 1−12.
(20) Lv, Y.; Yu, X.; Jia, J.; Tu, S. T.; Yan, J.; Dahlquist, E. Fabrication and Characterization of Superhydrophobic Polypropylene Hollow Fiber Membranes for Carbon Dioxide Absorption. *Appl. Energy* **2012**, *90* (1), 167−174.
(21) Wang, R.; Zhang, H. Y.; Feron, P. H. M.; Liang, D. T. Influence of Membrane Wetting on CO2 Capture in Microporous Hollow Fiber Membrane Contactors. *Sep. Purif. Technol.* **2005**, *46* (1−2), 33−40.
(22) Shao, J.; Liu, H.; He, Y. Boiler Feed Water Deoxygenation Using Hollow Fiber Membrane Contactor. *Desalination* **2008**, *234* (1−3), 370−377.
(23) Henares, M.; Ferrero, P.; San-Valero, P.; Martínez-Soria, V.; Izquierdo, M. Performance of a Polypropylene Membrane Contactor for the Recovery of Dissolved Methane from Anaerobic Effluents: Mass Transfer Evaluation, Long-Term Operation and Cleaning Strategies. *J. Membr. Sci.* **2018**, *563*, 926−937.
(24) Rongwong, W.; Goh, K.; Sethunga, G. S. M. D. P.; Bae, T. H. Fouling Formation in Membrane Contactors for Methane Recovery from Anaerobic Effluents. *J. Membr. Sci.* **2019**, *573*, 534−543.
(25) Darestani, M.; Haigh, V.; Couperthwaite, S. J.; Millar, G. J.; Nghiem, L. D. Hollow Fibre Membrane Contactors for Ammonia Recovery: Current Status and Future Developments. *J. Environ. Chem. Eng.* **2017**, *5* (2), 1349−1359.
(26) Gryta, M.; Tomaszewska, M.; Grzechulska, J.; Morawski, a. W. Membrane Distillation of NaCl Solution Containing Natural Organic Matter. *J. Membr. Sci.* **2001**, *181* (2), 279−287.
(27) Hausmann, A.; Sanciolo, P.; Vasiljevic, T.; Weeks, M.; Schroën, K.; Gray, S.; Duke, M. Fouling of Dairy Components on Hydrophobic Polytetrafluoroethylene (PTFE) Membranes for Membrane Distillation. *J. Membr. Sci.* **2013**, *442*, 149−159.
(28) Lin, S.; Nejati, S.; Boo, C.; Hu, Y.; Osuji, C. O.; Elimelech, M. Omniphobic Membrane for Robust Membrane Distillation. *Environ. Sci. Technol. Lett.* **2014**, *1* (11), 443−447.
(29) Wang, Z.; Chen, Y.; Sun, X.; Duddu, R.; Lin, S. Mechanism of Pore Wetting in Membrane Distillation with Alcohol vs. Surfactant. *J. Membr. Sci.* **2018**, *559*, 183−195.
(30) Chew, N. G. P.; Zhao, S.; Loh, C. H.; Permogorov, N.; Wang, R. Surfactant Effects on Water Recovery from Produced Water via Direct-Contact Membrane Distillation. *J. Membr. Sci.* **2017**, *528*, 126−134.

(31) Wang, Z.; Chen, Y.; Lin, S. Kinetic Model for Surfactant-Induced Pore Wetting in Membrane Distillation. *J. Membr. Sci.* **2018**, *564*, 275−288.
(32) Wang, Z.; Chen, Y.; Zhang, F.; Lin, S. Significance of Surface Excess Concentration in the Kinetics of Surfactant-Induced Pore Wetting in Membrane Distillation. *Desalination* **2019**, *450*, 46−53.
(33) Karakulski, K.; Gryta, M. Water Demineralisation by NF/MD Integrated Processes. *Desalination* **2005**, *177* (1−3), 109−119.
(34) He, F.; Gilron, J.; Lee, H.; Song, L.; Sirkar, K. K. Potential for Scaling by Sparingly Soluble Salts in Crossflow DCMD. *J. Membr. Sci.* **2008**, *311* (1−2), 68−80.
(35) Christie, K. S. S.; Yin, Y.; Lin, S.; Tong, T. Distinct Behaviors between Gypsum and Silica Scaling in Membrane Distillation. *Environ. Sci. Technol.* **2019**, *54* (1), 568−576.
(36) Gryta, M. Fouling in Direct Contact Membrane Distillation Process. *J. Membr. Sci.* **2008**, *325* (1), 383−394.
(37) Warsinger, D. M.; Swaminathan, J.; Guillen-Burrieza, E.; Arafat, H. A.; Lienhard V, J. H. Scaling and Fouling in Membrane Distillation for Desalination Applications: A Review. *Desalination* **2015**, *356*, 294−313.
(38) Wang, Z.; Lin, S. Membrane Fouling and Wetting in Membrane Distillation and Their Mitigation by Novel Membranes with Special Wettability. *Water Res.* **2017**, *112*, 38−47.
(39) Guillen-Burrieza, E.; Mavukkandy, M. O.; Bilad, M. R.; Arafat, H. A. Understanding Wetting Phenomena in Membrane Distillation and How Operational Parameters Can Affect It. *J. Membr. Sci.* **2016**, *515*, 163−174.
(40) Guillen-Burrieza, E.; Ruiz-Aguirre, A.; Zaragoza, G.; Arafat, H. A. Membrane Fouling and Cleaning in Long Term Plant-Scale Membrane Distillation Operations. *J. Membr. Sci.* **2014**, *468*, 360−372.
(41) Rezaei, M.; Warsinger, D. M.; Lienhard V, J. H.; Duke, M. C.; Matsuura, T.; Samhaber, W. M. Wetting Phenomena in Membrane Distillation: Mechanisms, Reversal, and Prevention. *Water Res.* **2018**, *139*, 329−352.
(42) Gryta, M. Long-Term Performance of Membrane Distillation Process. *J. Membr. Sci.* **2005**, *265* (1−2), 153−159.
(43) Lu, J. G.; Zheng, Y. F.; Cheng, M. D. Wetting Mechanism in Mass Transfer Process of Hydrophobic Membrane Gas Absorption. *J. Membr. Sci.* **2008**, *308* (1−2), 180−190.
(44) Gabelman, A.; Hwang, S. T. Hollow Fiber Membrane Contactors. *J. Membr. Sci.* **1999**, *159* (1−2), 61−106.
(45) Kreulen, H.; Smolders, C. A.; Versteeg, G. F.; Van Swaaij, W. P. M. Determination of Mass Transfer Rates in Wetted and Non-Wetted Microporous Membranes. *Chem. Eng. Sci.* **1993**, *48* (11), 2093−2102.
(46) Gryta, M.; Barancewicz, M. Influence of Morphology of PVDF Capillary Membranes on the Performance of Direct Contact Membrane Distillation. *J. Membr. Sci.* **2010**, *358* (1−2), 158−167.
(47) Chen, Y.; Wang, Z.; Jennings, G. K.; Lin, S. Probing Pore Wetting in Membrane Distillation Using Impedance: Early Detection and Mechanism of Surfactant-Induced Wetting. *Environ. Sci. Technol. Lett.* **2017**, *4* (11), 505−510.
(48) Jacob, P.; Dejean, B.; Laborie, S.; Cabassud, C. An Optical In-Situ Tool for Visualizing and Understanding Wetting Dynamics in Membrane Distillation. *J. Membr. Sci.* **2020**, *595*, 117587.
(49) Tuberquia, J. C.; Song, W. S.; Jennings, G. K. Investigating the Superhydrophobic Behavior for Underwater Surfaces Using Impedance-Based Methods. *Anal. Chem.* **2011**, *83* (16), 6184−6190.
(50) Tuberquia, J. C.; Nizamidin, N.; Jennings, G. K. Effect of Superhydrophobicity on the Barrier Properties of Polymethylene Films. *Langmuir* **2010**, *26* (17), 14039−14046.
(51) Franken, A. C. M.; Nolten, J. A. M.; Mulder, M. H. V; Bargeman, D.; Smolders, C. A. Wetting Criteria for the Applicability of Membrane Distillation. *J. Membr. Sci.* **1987**, *33* (3), 315−328.
(52) García-Payo, M. C.; Izquierdo-Gil, M. A.; Fernández-Pineda, C. Wetting Study of Hydrophobic Membranes via Liquid Entry Pressure Measurements with Aqueous Alcohol Solutions. *J. Colloid Interface Sci.* **2000**, *230*, 420−431.
(53) Jacob, P.; Laborie, S.; Cabassud, C. Visualizing and Evaluating Wetting in Membrane Distillation: New Methodology and Indicators Based on Detection of Dissolved Tracer Intrusion (DDTI). *Desalination* **2018**, *443*, 307−322.
(54) Zmievskii, Y. G. Determination of Critical Pressure in Membrane Distillation Process. *Pet. Chem.* **2015**, *55* (4), 308−314.
(55) Churaev, N. V.; Martynov, G. A.; Starov, V. M.; Zorin, Z. M. Some Features of Capillary Imbibition of Surfactant Solutions. *Colloid Polym. Sci.* **1981**, *259*, 747−752.
(56) Starov, V. M.; Zhdanov, S. A.; Velarde, M. G. Capillary Imbibition of Surfactant Solutions in Porous Media and Thin Capillaries: Partial Wetting Case. *J. Colloid Interface Sci.* **2004**, *273* (2), 589−595.
(57) Rosen, M. J.; Cohen, A. W.; Dahanayake, M.; Hua, X. Y. Relationship of Structure to Properties in Surfactants. 10. Surface and Thermodynamic Properties of 2-Dodecyloxypoly(Ethenoxyethanol)s, C12H25(OC2H4)XOH, in Aqueous Solution. *J. Phys. Chem.* **1982**, *86* (4), 541−545.
(58) Dong, B.; Li, N.; Zheng, L.; Yu, L.; Inoue, T. Surface Adsorption and Micelle Formation of Surface Active Ionic Liquids in Aqueous Solution. *Langmuir* **2007**, *23* (8), 4178−4182.
(59) Adamson, A. W.; Gast, A. P. Physical Chemistry of Surfaces. *Z. Phys. Chem.* **1967**, *150*, 134.
(60) Tan, Y. Z.; Velioglu, S.; Han, L.; Joseph, B. D.; Unnithan, L. G.; Chew, J. W. Effect of Surfactant Hydrophobicity and Charge Type on Membrane Distillation Performance. *J. Membr. Sci.* **2019**, *587*, 117168.
(61) Milne, A. J. B.; Amirfazli, A. Autophilic Effect: Wetting of Hydrophobic Surfaces by Surfactant Solutions. *Langmuir* **2010**, *26* (7), 4668−4674.
(62) Kumar, N.; Varanasi, K.; Tilton, R. D.; Garoff, S. Surfactant Self-Assembly Ahead of the Contact Line on a Hydrophobic Surface and Its Implications for Wetting. *Langmuir* **2003**, *19* (13), 5366−5373.
(63) Bailey, A. F. G.; Barbe, A. M.; Hogan, P. A.; Johnson, R. A.; Sheng, J. The Effect of Ultrafiltration on the Subsequent Concentration of Grape Juice by Osmotic Distillation. *J. Membr. Sci.* **2000**, *164* (1−2), 195−204.
(64) Zarebska, A.; Amor, Á. C.; Ciurkot, K.; Karring, H.; Thygesen, O.; Andersen, T. P.; Hägg, M. B.; Christensen, K. V.; Norddahl, B. Fouling Mitigation in Membrane Distillation Processes during Ammonia Stripping from Pig Manure. *J. Membr. Sci.* **2015**, *484*, 119−132.
(65) Kowalska, I. Nanofiltration -Ion Exchange System for Effective Surfactant Removal from Water Solutions. *Braz. J. Chem. Eng.* **2014**, *31* (4), 887−894.
(66) Beltrán-Heredia, J.; Sánchez-Martín, J.; Barrado-Moreno, M. Long-Chain Anionic Surfactants in Aqueous Solution. Removal by Moringa Oleifera Coagulant. *Chem. Eng. J.* **2012**, *180*, 128−136.
(67) Aboulhassan, M. A.; Souabi, S.; Yaacoubi, A.; Baudu, M. Removal of Surfactant from Industrial Wastewaters by Coagulation Flocculation Process. *Int. J. Environ. Sci. Technol.* **2006**, *3* (4), 327−332.
(68) Chen, S.; Timmons, M. B.; Bisogni, J. J.; Aneshansley, D. J. Modeling Surfactant Removal in Foam Fractionation: I - Theoretical Development. *Aquac. Eng.* **1994**, *13* (3), 163−181.
(69) Lee, J.; Maa, J. R. Separation of a Surface Active Solute by Foam Fractionation. *Int. Commun. Heat Mass Transfer* **1986**, *13*, 465−473.
(70) Dow, N.; Villalobos García, J.; Niadoo, L.; Milne, N.; Zhang, J.; Gray, S.; Duke, M. Demonstration of Membrane Distillation on Textile Waste Water Assessment of Long Term Performance, Membrane Cleaning and Waste Heat Integration. *Environ. Sci. Water Res. Technol.* **2017**, *3* (3), 433−449.
(71) Camacho-Muñoz, D.; Martín, J.; Santos, J. L.; Aparicio, I.; Alonso, E. Occurrence of Surfactants in Wastewater: Hourly and Seasonal Variations in Urban and Industrial Wastewaters from Seville (Southern Spain). *Sci. Total Environ.* **2014**, *468−469*, 977−984.

https://dx.doi.org/10.1021/acsestengg.0c00025
ACS EST Engg. 2021, 1, 117−140

(72) Chen, H. J.; Tseng, D. H.; Huang, S. L. Biodegradation of Octylphenol Polyethoxylate Surfactant Triton X-100 by Selected Microorganisms. *Bioresour. Technol.* **2005**, *96* (13), 1483−1491.
(73) Boo, C.; Lee, J.; Elimelech, M. Omniphobic Polyvinylidene Fluoride (PVDF) Membrane for Desalination of Shale Gas Produced Water by Membrane Distillation. *Environ. Sci. Technol.* **2016**, *50* (22), 12275−12282.
(74) Chul Woo, Y.; Chen, Y.; Tijing, L. D.; Phuntsho, S.; He, T.; Choi, J. S.; Kim, S. H.; Kyong Shon, H. CF4 Plasma-Modified Omniphobic Electrospun Nanofiber Membrane for Produced Water Brine Treatment by Membrane Distillation. *J. Membr. Sci.* **2017**, *529*, 234−242.
(75) Lee, J.; Boo, C.; Ryu, W. H.; Taylor, A. D.; Elimelech, M. Development of Omniphobic Desalination Membranes Using a Charged Electrospun Nanofiber Scaffold. *ACS Appl. Mater. Interfaces* **2016**, *8* (17), 11154−11161.
(76) Li, J.; Guo, S.; Xu, Z.; Li, J.; Pan, Z.; Du, Z.; Cheng, F. Preparation of Omniphobic PVDF Membranes with Silica Nanoparticles for Treating Coking Wastewater Using Direct Contact Membrane Distillation: Electrostatic Adsorption vs. Chemical Bonding. *J. Membr. Sci.* **2019**, *574*, 349−357.
(77) Chen, L. H.; Huang, A.; Chen, Y. R.; Chen, C. H.; Hsu, C. C.; Tsai, F. Y.; Tung, K. L. Omniphobic Membranes for Direct Contact Membrane Distillation: Effective Deposition of Zinc Oxide Nanoparticles. *Desalination* **2018**, *428*, 255−263.
(78) Lu, K. J.; Zuo, J.; Chang, J.; Kuan, H. N.; Chung, T. S. Omniphobic Hollow-Fiber Membranes for Vacuum Membrane Distillation. *Environ. Sci. Technol.* **2018**, *52* (7), 4472−4480.
(79) Lu, C.; Su, C.; Cao, H.; Ma, X.; Duan, F.; Chang, J.; Li, Y. F-POSS Based Omniphobic Membrane for Robust Membrane Distillation. *Mater. Lett.* **2018**, *228*, 85−88.
(80) Zheng, R.; Chen, Y.; Wang, J.; Song, J.; Li, X. M.; He, T. Preparation of Omniphobic PVDF Membrane with Hierarchical Structure for Treating Saline Oily Wastewater Using Direct Contact Membrane Distillation. *J. Membr. Sci.* **2018**, *555*, 197−205.
(81) Deng, L.; Ye, H.; Li, X.; Li, P.; Zhang, J.; Wang, X.; Zhu, M.; Hsiao, B. S. Self-Roughened Omniphobic Coatings on Nanofibrous Membrane for Membrane Distillation. *Sep. Purif. Technol.* **2018**, *206*, 14−25.
(82) Lu, K. J.; Chen, Y.; Chung, T. S. Design of Omniphobic Interfaces for Membrane Distillation − A Review. *Water Res.* **2019**, *162*, 64−77.
(83) Tuteja, A.; Choi, W.; Ma, M.; Mabry, J. M.; Mazzella, S. a; Rutledge, G. C.; McKinley, G. H.; Cohen, R. E. Designing Superoleophobic Surfaces. *Science* **2007**, *318* (5856), 1618−1622.
(84) Tuteja, A.; Choi, W.; Mabry, J. M.; McKinley, G. H.; Cohen, R. E. Robust Omniphobic Surfaces. *Proc. Natl. Acad. Sci. U. S. A.* **2008**, *105* (47), 18200−18205.
(85) Dufour, R.; Harnois, M.; Thomy, V.; Boukherroub, R.; Senez, V. Contact Angle Hysteresis Origins: Investigation on Super-Omniphobic Surfaces. *Soft Matter* **2011**, *7* (19), 9380−9387.
(86) Chhatre, S. S.; Choi, W.; Tuteja, A.; Park, K. C.; Mabry, J. M.; McKinley, G. H.; Cohen, R. E. Scale Dependence of Omniphobic Mesh Surfaces. *Langmuir* **2010**, *26* (6), 4027−4035.
(87) Boo, C.; Lee, J.; Elimelech, M. Engineering Surface Energy and Nanostructure of Microporous Films for Expanded Membrane Distillation Applications. *Environ. Sci. Technol.* **2016**, *50* (15), 8112−8119.
(88) Wang, W.; Du, X.; Vahabi, H.; Zhao, S.; Yin, Y.; Kota, A. K.; Tong, T. Trade-off in Membrane Distillation with Monolithic Omniphobic Membranes. *Nat. Commun.* **2019**, *10* (1), 1−9.
(89) Liu, T.; Kim, C.-J. Turning a Surface Superrepellent Even to Completely Wetting Liquids. *Science* **2014**, *346* (6213), 1096−1100.
(90) Yao, M.; Tijing, L. D.; Naidu, G.; Kim, S. H.; Matsuyama, H.; Fane, A. G.; Shon, H. K. A Review of Membrane Wettability for the Treatment of Saline Water Deploying Membrane Distillation. *Desalination* **2020**, *479*, 114312.
(91) Burton, F.; Tsuchihasi, R.; Tchobanoglous, G.; Stensel, H. D. *Wastewater Engineering: Treatment and Resource Recovery*, 5th ed.; McGraw-Hill Education, 2013.
(92) Gryta, M. Studies of Membrane Scaling during Water Desalination by Membrane Distillation. *Chem. Pap.* **2019**, *73* (3), 591−600.
(93) McGaughey, A. L.; Gustafson, R. D.; Childress, A. E. Effect of Long-Term Operation on Membrane Surface Characteristics and Performance in Membrane Distillation. *J. Membr. Sci.* **2017**, *543*, 143−150.
(94) Ramezanianpour, M.; Sivakumar, M. An Analytical Flux Decline Model for Membrane Distillation. *Desalination* **2014**, *345*, 1−12.
(95) Karanikola, V.; Boo, C.; Rolf, J.; Elimelech, M. Engineered Slippery Surface to Mitigate Gypsum Scaling in Membrane Distillation for Treatment of Hypersaline Industrial Wastewaters. *Environ. Sci. Technol.* **2018**, *52* (24), 14362−14370.
(96) Su, C.; Horseman, T.; Cao, H.; Christie, K.; Li, Y.; Lin, S. Robust Superhydrophobic Membrane for Membrane Distillation with Excellent Scaling Resistance. *Environ. Sci. Technol.* **2019**, *53* (20), 11801−11809.
(97) Xie, M.; Gray, S. R. Gypsum Scaling in Forward Osmosis: Role of Membrane Surface Chemistry. *J. Membr. Sci.* **2016**, *513*, 250−259.
(98) Fortunato, L.; Jang, Y.; Lee, J. G.; Jeong, S.; Lee, S.; Leiknes, T. O.; Ghaffour, N. Fouling Development in Direct Contact Membrane Distillation: Non-Invasive Monitoring and Destructive Analysis. *Water Res.* **2018**, *132*, 34−41.
(99) Lee, J.-G.; Jang, Y.; Fortunato, L.; Jeong, S.; Lee, S.; Leiknes, T.; Ghaffour, N. An Advanced Online Monitoring Approach to Study the Scaling Behavior in Direct Contact Membrane Distillation. *J. Membr. Sci.* **2018**, *546*, 50−60.
(100) Lokare, O. R.; Ji, P.; Wadekar, S.; Dutt, G.; Vidic, R. D. Concentration Polarization in Membrane Distillation: I. Development of a Laser-Based Spectrophotometric Method for in-Situ Characterization. *J. Membr. Sci.* **2019**, *581*, 462−471.
(101) Gibbs, J. W. On the Equilibrium of Heterogeneous Substances. *Am. J. Sci.* **1879**, *2*, 300−320.
(102) Tong, T.; Wallace, A. F.; Zhao, S.; Wang, Z. Mineral Scaling in Membrane Desalination: Mechanisms, Mitigation Strategies, and Feasibility of Scaling-Resistant Membranes. *J. Membr. Sci.* **2019**, *579*, 52−69.
(103) Tong, T.; Zhao, S.; Boo, C.; Hashmi, S. M.; Elimelech, M. Relating Silica Scaling in Reverse Osmosis to Membrane Surface Properties. *Environ. Sci. Technol.* **2017**, *51* (8), 4396−4406.
(104) Giuffre, A. J.; Hamm, L. M.; Han, N.; De Yoreo, J. J.; Dove, P. M. Polysaccharide Chemistry Regulates Kinetics of Calcite Nucleation through Competition of Interfacial Energies. *Proc. Natl. Acad. Sci. U. S. A.* **2013**, *110* (23), 9261−9266.
(105) Hamm, L. M.; Giuffre, A. J.; Han, N.; Tao, J.; Wang, D.; De Yoreo, J. J.; Dove, P. M. Reconciling Disparate Views of Template-Directed Nucleation through Measurement of Calcite Nucleation Kinetics and Binding Energies. *Proc. Natl. Acad. Sci. U. S. A.* **2014**, *111* (4), 1304−1309.
(106) Rahardianto, A.; Mccool, B. C.; Cohen, Y. Reverse Osmosis Desalting of Inland Brackish Water of High Gypsum Scaling Propensity: Kinetics and Mitigation of Membrane Mineral Scaling. *Environ. Sci. Technol.* **2008**, *42* (12), 4292−4297.
(107) Wu, W.; Nancollas, G. H. Interfacial Free Energies and Crystallization in Aqueous Media. *J. Colloid Interface Sci.* **1996**, *182* (2), 365−373.
(108) Van Oss, C. J.; Chaudhury, M. K.; Good, R. J. Interfacial Lifshitz-van Der Waals and Polar Interactions in Macroscopic Systems. *Chem. Rev.* **1988**, *88* (6), 927−941.
(109) Israelachvili, J. *Intermolecular and Surface Forces*, 3rd ed.; Science Direct, 2010. DOI: 10.1016/B978-0-12-375182-9.10025-9.
(110) Chibowski, E.; Holysz, L. Use of the Washburn Equation for Surface Free Energy Determination. *Langmuir* **1992**, *8* (2), 710−716.

(111) Teng, F.; Zeng, H.; Liu, Q. Understanding the Deposition and Surface Interactions of Gypsum. *J. Phys. Chem. C* **2011**, *115* (35), 17485−17494.
(112) Zheng, R.; Yin, H.; Liu, Y.; He, H.; Zhang, Y.; Li, X.-M.; Ji, Y.; Xiao, Z.; Yuan, X.; He, T.; Li, D. Slippery for Scaling Resistance in Membrane Distillation: A Novel Porous Micropillared Superhydrophobic Surface. *Water Res.* **2019**, *155*, 152−161.
(113) Xiao, Z.; Li, Z.; Guo, H.; Liu, Y.; Wang, Y.; Yin, H.; Li, X.; Song, J.; Nghiem, L. D.; He, T. Scaling Mitigation in Membrane Distillation: From Superhydrophobic to Slippery. *Desalination* **2019**, *466*, 36−43.
(114) Martínez-Díez, L.; Vázquez-González, M. Temperature and Concentration Polarization in Membrane Distillation of Aqueous Salt Solutions. *J. Membr. Sci.* **1999**, *156* (2), 265−273.
(115) Gilron, J.; Ladizansky, Y.; Korin, E. Silica Fouling in Direct Contact Membrane Distillation. *Ind. Eng. Chem. Res.* **2013**, *52* (31), 10521−10529.
(116) Tun, C. M.; Fane, A. G.; Matheickal, J. T.; Sheikholeslami, R. Membrane Distillation Crystallization of Concentrated Salts — Flux and Crystal Formation. *J. Membr. Sci.* **2005**, *257*, 144−155.
(117) Warsinger, D. M.; Tow, E. W.; Swaminathan, J.; Lienhard V, J. H. Theoretical Framework for Predicting Inorganic Fouling in Membrane Distillation and Experimental Validation with Calcium Sulfate. *J. Membr. Sci.* **2017**, *528*, 381−390.
(118) Fein, J. B.; Walther, J. V. Calcite Solubility in Supercritical CO2H2O Fluids. *Geochim. Cosmochim. Acta* **1987**, *51* (6), 1665−1673.
(119) Azimi, G. *Evaluating the Potential of Scaling Due to Calcium Compounds in Hydrometallurgical Processes*, Ph.D. Thesis; University of Toronto, 2010.
(120) He, S.; Oddo, J. E.; Tomson, M. B. The Nucleation Kinetics of Calcium Sulfate Dihydrate in NaCl Solutions up to 6 m and 90°C. *J. Colloid Interface Sci.* **1994**, *162* (2), 297−303.
(121) Yin, Y.; Wang, W.; Kota, A. K.; Zhao, S.; Tong, T. Elucidating Mechanisms of Silica Scaling in Membrane Distillation: Effects of Membrane Surface Wettability. *Environ. Sci. Water Res. Technol.* **2019**, *5* (11), 2004−2014.
(122) Warsinger, C.; Martin, D.; Swaminathan, J.; Chung, H. W.; Jeong, S.; Lienhard, J. H.; Martin Warsinger, D.; Warsinger, D. M. Effect of Filtration and Particulate Fouling in Membrane Distillation. *International Desalination Association* **2015**, 0−14.
(123) Barbe, A. M.; Hogan, P. A.; Johnson, R. A. Surface Morphology Changes during Initial Usage of Hydrophobic, Microporous Polypropylene Membranes. *J. Membr. Sci.* **2000**, *172* (1−2), 149−156.
(124) Gryta, M. Influence of Polypropylene Membrane Surface Porosity on the Performance of Membrane Distillation Process. *J. Membr. Sci.* **2007**, *287* (1), 67−78.
(125) Andrés-Mañas, J. A.; Ruiz-Aguirre, A.; Acién, F. G.; Zaragoza, G. Assessment of a Pilot System for Seawater Desalination Based on Vacuum Multi-Effect Membrane Distillation with Enhanced Heat Recovery. *Desalination* **2018**, *443*, 110−121.
(126) Yu, X.; Yang, H.; Lei, H.; Shapiro, A. Experimental Evaluation on Concentrating Cooling Tower Blowdown Water by Direct Contact Membrane Distillation. *Desalination* **2013**, *323*, 134−141.
(127) Peng, Y.; Ge, J.; Li, Z.; Wang, S. Effects of Anti-Scaling and Cleaning Chemicals on Membrane Scale in Direct Contact Membrane Distillation Process for RO Brine Concentrate. *Sep. Purif. Technol.* **2015**, *154*, 22−26.
(128) He, F.; Sirkar, K. K.; Gilron, J. Effects of Antiscalants to Mitigate Membrane Scaling by Direct Contact Membrane Distillation. *J. Membr. Sci.* **2009**, *345*, 53−58.
(129) Qu, F.; Yan, Z.; Yu, H.; Fan, G.; Pang, H.; Rong, H.; He, J. Effect of Residual Commercial Antiscalants on Gypsum Scaling and Membrane Wetting during Direct Contact Membrane Distillation. *Desalination* **2020**, *486*, 114493.
(130) Minier-Matar, J.; Hussain, A.; Janson, A.; Benyahia, F.; Adham, S. Field Evaluation of Membrane Distillation Technologies for Desalination of Highly Saline Brines. *Desalination* **2014**, *351*, 101−108.
(131) Hou, D.; Dai, G.; Wang, J.; Fan, H.; Luan, Z.; Fu, C. Boron Removal and Desalination from Seawater by PVDF Flat-Sheet Membrane through Direct Contact Membrane Distillation. *Desalination* **2013**, *326*, 115−124.
(132) Gryta, M. Polyphosphates Used for Membrane Scaling Inhibition during Water Desalination by Membrane Distillation. *Desalination* **2012**, *285*, 170−176.
(133) Zhang, P.; Knötig, P.; Gray, S.; Duke, M. Scale Reduction and Cleaning Techniques during Direct Contact Membrane Distillation of Seawater Reverse Osmosis Brine. *Desalination* **2015**, *374*, 20−30.
(134) Gryta, M.; Tomaszewska, M.; Karakulski, K. Wastewater Treatment by Membrane Distillation. *Desalination* **2006**, *198* (1−3), 67−73.
(135) Zhang, P.; Pabstmann, A.; Gray, S.; Duke, M. Silica Fouling during Direct Contact Membrane Distillation of Coal Seam Gas Brine with High Sodium Bicarbonate and Low Hardness. *Desalination* **2018**, *444*, 107−117.
(136) Sun, X.; Zhang, J.; Yin, C.; Zhang, J.; Han, J. Poly(Aspartic Acid)-Tryptophan Grafted Copolymer and Its Scale-Inhibition Performance. *J. Appl. Polym. Sci.* **2015**, *132* (45), 2−9.
(137) Duan, W.; Oota, H.; Sawada, K. Stability and Structure of Ethylenedinitrilopoly(Methylphosphonate) Complexes of the Alkaline-Earth Metal Ions in Aqueous Solution. *J. Chem. Soc., Dalton Trans.* **1999**, *493* (17), 3075−3080.
(138) Deluchat, V.; Bollinger, J. C.; Serpaud, B.; Caullet, C. Divalent Cations Speciation with Three Phosphonate Ligands in the PH-Range of Natural Waters. *Talanta* **1997**, *44* (5), 897−907.
(139) Lioliou, M. G.; Paraskeva, C. A.; Koutsoukos, P. G.; Payatakes, A. C. Calcium Sulfate Precipitation in the Presence of Water-Soluble Polymers. *J. Colloid Interface Sci.* **2006**, *303* (1), 164−170.
(140) Battaglia, G.; Crea, F.; Crea, P.; Sammartano, S. The Protonation of Polyacrylate in Seawater. Analysis of Concentration Effects. *Ann. Chim.* **2005**, *95* (9−10), 643−656.
(141) Liu, Z.; Wang, S.; Zhang, L.; Liu, Z. Dynamic Synergistic Scale Inhibition Performance of IA/SAS/SHP Copolymer with Magnetic Field and Electrostatic Field. *Desalination* **2015**, *362*, 26−33.
(142) Ahmed, S. B.; Tlili, M. M.; Amor, M. B. Influence of a Polyacrylate Antiscalant on Gypsum Nucleation and Growth. *Cryst. Res. Technol.* **2008**, *43* (9), 935−942.
(143) Shih, W. Y.; Albrecht, K.; Glater, J.; Cohen, Y. A Dual-Probe Approach for Evaluation of Gypsum Crystallization in Response to Antiscalant Treatment. *Desalination* **2004**, *169* (3), 213−221.
(144) Le Gouellec, Y. A.; Elimelech, M. Control of Calcium Sulfate (Gypsum) Scale in Nanofiltration of Saline Agricultural Drainage Water. *Environ. Eng. Sci.* **2002**, *19* (6), 387−397.
(145) Jain, T.; Sanchez, E.; Owens-Bennett, E.; Trussell, R.; Walker, S.; Liu, H. Impacts of Antiscalants on the Formation of Calcium Solids: Implication on Scaling Potential of Desalination Concentrate. *Environ. Sci. Water Res. Technol.* **2019**, *5* (7), 1285−1294.
(146) Shih, W. Y.; Gao, J.; Rahardianto, A.; Glater, J.; Cohen, Y.; Gabelich, C. J. Ranking of Antiscalant Performance for Gypsum Scale Suppression in the Presence of Residual Aluminum. *Desalination* **2006**, *196* (1−3), 280−292.
(147) Rabizadeh, T.; Morgan, D. J.; Peacock, C. L.; Benning, L. G. Effectiveness of Green Additives vs Poly(Acrylic Acid) in Inhibiting Calcium Sulfate Dihydrate Crystallization. *Ind. Eng. Chem. Res.* **2019**, *58* (4), 1561−1569.
(148) Oh, H. J.; Choung, Y. K.; Lee, S.; Choi, J. S.; Hwang, T. M.; Kim, J. H. Scale Formation in Reverse Osmosis Desalination: Model Development. *Desalination* **2009**, *238* (1−3), 333−346.
(149) Weijnen, M. P. C.; Van Rosmalen, G. M. Adsorption of Phosphonates on Gypsum Crystals. *J. Cryst. Growth* **1986**, *79* (1−3), 157−168.
(150) Rosenberg, Y. O.; Reznik, I. J.; Zmora-Nahum, S.; Ganor, J. The Effect of PH on the Formation of a Gypsum Scale in the Presence of a Phosphonate Antiscalant. *Desalination* **2012**, *284*, 207−220.

https://dx.doi.org/10.1021/acsestengg.0c00025
ACS EST Engg. 2021, 1, 117−140

(151) Wang, J.; Qu, D.; Tie, M.; Ren, H.; Peng, X.; Luan, Z. Effect of Coagulation Pretreatment on Membrane Distillation Process for Desalination of Recirculating Cooling Water. *Sep. Purif. Technol.* **2008**, *64* (1), 108−115.
(152) Zhang, Z.; Du, X.; Carlson, K. H.; Robbins, C. A.; Tong, T. Effective Treatment of Shale Oil and Gas Produced Water by Membrane Distillation Coupled with Precipitative Softening and Walnut Shell Filtration. *Desalination* **2019**, *454*, 82−90.
(153) Yang, C.; Li, X. M.; Gilron, J.; Kong, D.-F.; Yin, Y.; Oren, Y.; Linder, C.; He, T. CF4 Plasma-Modified Superhydrophobic PVDF Membranes for Direct Contact Membrane Distillation. *J. Membr. Sci.* **2014**, *456*, 155−161.
(154) Zhang, W.; Li, Y.; Liu, J.; Li, B.; Wang, S. Fabrication of Hierarchical Poly (Vinylidene Fluoride) Micro/Nano-Composite Membrane with Anti-Fouling Property for Membrane Distillation. *J. Membr. Sci.* **2017**, *535*, 258−267.
(155) Milne, A. J. B.; Amirfazli, A. The Cassie Equation: How It Is Meant to Be Used. *Adv. Colloid Interface Sci.* **2012**, *170* (1−2), 48−55.
(156) Meng, S.; Ye, Y.; Mansouri, J.; Chen, V. Crystallization Behavior of Salts during Membrane Distillation with Hydrophobic and Superhydrophobic Capillary Membranes. *J. Membr. Sci.* **2015**, *473*, 165−176.
(157) Ye, Y.; Yu, S.; Hou, L.; Liu, B.; Xia, Q.; Liu, G.; Li, P. Microbubble Aeration Enhances Performance of Vacuum Membrane Distillation Desalination by Alleviating Membrane Scaling. *Water Res.* **2019**, *149*, 588−595.
(158) Rao, U.; Iddya, A.; Jung, B.; Khor, C. M.; Hendren, Z.; Turchi, C.; Cath, T.; Hoek, E. M. V.; Ramon, G. Z.; Jassby, D. Mineral Scale Prevention on Electrically Conducting Membrane Distillation Membranes Using Induced Electrophoretic Mixing. *Environ. Sci. Technol.* **2020**, *54* (6), 3678−3690.
(159) Hickenbottom, K. L.; Cath, T. Y. Sustainable Operation of Membrane Distillation for Enhancement of Mineral Recovery from Hypersaline Solutions. *J. Membr. Sci.* **2014**, *454*, 426−435.
(160) Zou, T.; Kang, G.; Zhou, M.; Li, M.; Cao, Y. Submerged Vacuum Membrane Distillation Crystallization (S-VMDC) with Turbulent Intensification for the Concentration of NaCl Solution. *Sep. Purif. Technol.* **2019**, *211*, 151−161.
(161) Edwie, F.; Chung, T. S. Development of Simultaneous Membrane Distillation-Crystallization (SMDC) Technology for Treatment of Saturated Brine. *Chem. Eng. Sci.* **2013**, *98*, 160−172.
(162) Curcio, E.; Drioli, E. Membrane Distillation and Related Operations - A Review. *Sep. Purif. Rev.* **2005**, *34* (1), 35−86.
(163) Choi, Y.; Naidu, G.; Nghiem, L. D.; Lee, S.; Vigneswaran, S. Membrane Distillation Crystallization for Brine Mining and Zero Liquid Discharge: Opportunities, Challenges, and Recent Progress. *Environ. Sci. Water Res. Technol.* **2019**, *5* (7), 1202−1221.
(164) Anisi, F.; Thomas, K. M.; Kramer, H. J. M. Membrane-Assisted Crystallization: Membrane Characterization, Modelling and Experiments. *Chem. Eng. Sci.* **2017**, *158*, 277−286.
(165) Ruiz Salmón, I.; Luis, P. Membrane Crystallization via Membrane Distillation. *Chem. Eng. Process.* **2018**, *123*, 258−271.
(166) Gryta, M. Chemical Pretreatment of Feed Water for Membrane Distillation. *Chem. Pap.* **2008**, *62* (1), 100−105.
(167) Luo, L.; Zhao, J.; Chung, T.-S. Integration of Membrane Distillation (MD) and Solid Hollow Fiber Cooling Crystallization (SHFCC) Systems for Simultaneous Production of Water and Salt Crystals. *J. Membr. Sci.* **2018**, *564*, 905−915.
(168) Macedonio, F.; Curcio, E.; Drioli, E. Integrated Membrane Systems for Seawater Desalination: Energetic and Exergetic Analysis, Economic Evaluation, Experimental Study. *Desalination* **2007**, *203* (1−3), 260−276.
(169) Quist-Jensen, C. A.; Macedonio, F.; Horbez, D.; Drioli, E. Reclamation of Sodium Sulfate from Industrial Wastewater by Using Membrane Distillation and Membrane Crystallization. *Desalination* **2017**, *401*, 112−119.
(170) Kim, J.; Kim, J.; Hong, S. Recovery of Water and Minerals from Shale Gas Produced Water by Membrane Distillation Crystallization. *Water Res.* **2018**, *129*, 447−459.
(171) Shin, Y.; Sohn, J. Mechanisms for Scale Formation in Simultaneous Membrane Distillation Crystallization: Effect of Flow Rate. *J. Ind. Eng. Chem.* **2016**, *35*, 318−324.
(172) Chellam, S.; Jacangelo, J. G.; Bonacquisti, T. P. Modeling and Experimental Verification of Pilot-Scale Hollow Fiber, Direct Flow Microfiltration with Periodic Backwashing. *Environ. Sci. Technol.* **1998**, *32* (1), 75−81.
(173) Su, S. K.; Liu, J. C.; Wiley, R. C. Cross-Flow Microfiltration with Gas Backwash of Apple Juice. *J. Food Sci.* **1993**, *58* (3), 638−641.
(174) Horseman, T.; Su, C.; Christie, K. S. S.; Lin, S. Highly Effective Scaling Mitigation in Membrane Distillation Using a Superhydrophobic Membrane with Gas Purging. *Environ. Sci. Technol. Lett.* **2019**, *6* (7), 423−429.
(175) Liu, Y.; Li, Z.; Xiao, Z.; Yin, H.; Li, X.; He, T. Synergy of Slippery Surface and Pulse Flow: An Anti-Scaling Solution for Direct Contact Membrane Distillation. *J. Membr. Sci.* **2020**, *603*, 118035.
(176) Bogler, A.; Bar-Zeev, E. Membrane Distillation Biofouling: Impact of Feedwater Temperature on Biofilm Characteristics and Membrane Performance. *Environ. Sci. Technol.* **2018**, *52* (17), 10019−10029.
(177) Kwan, S. E.; Bar-Zeev, E.; Elimelech, M. Biofouling in Forward Osmosis and Reverse Osmosis: Measurements and Mechanisms. *J. Membr. Sci.* **2015**, *493*, 703−708.
(178) Yoon, H.; Baek, Y.; Yu, J.; Yoon, J. Biofouling Occurrence Process and Its Control in the Forward Osmosis. *Desalination* **2013**, *325*, 30−36.
(179) Israelachvili, J.; Pashley, R. The Hydrophobic Interaction Is Long Range, Decaying Exponentially with Distance. *Nature* **1982**, *300* (5890), 341−342.
(180) Meyer, E. E.; Rosenberg, K. J.; Israelachvili, J. Recent Progress in Understanding Hydrophobic Interactions. *Proc. Natl. Acad. Sci. U. S. A.* **2006**, *103* (43), 15739−15746.
(181) Ho, J. S.; Sim, L. N.; Webster, R. D.; Viswanath, B.; Coster, H. G. L.; Fane, A. G. Monitoring Fouling Behavior of Reverse Osmosis Membranes Using Electrical Impedance Spectroscopy: A Field Trial Study. *Desalination* **2017**, *407*, 75−84.
(182) Kavanagh, J. M.; Hussain, S.; Chilcott, T. C.; Coster, H. G. L. Fouling of Reverse Osmosis Membranes Using Electrical Impedance Spectroscopy: Measurements and Simulations. *Desalination* **2009**, *236* (1−3), 187−193.
(183) Ahmed, F. E.; Hilal, N.; Hashaikeh, R. Electrically Conductive Membranes for in Situ Fouling Detection in Membrane Distillation Using Impedance Spectroscopy. *J. Membr. Sci.* **2018**, *556*, 66−72.
(184) Zhang, N.; Halali, M. A.; de Lannoy, C.-F. Detection of Fouling on Electrically Conductive Membranes by Electrical Impedance Spectroscopy. *Sep. Purif. Technol.* **2020**, *242*, 116823.
(185) Tsao, Y.; Evans, D.; Wennerstrom, H. Long-Range Attractive Force between Hydrophobic Surfaces Observed by Atomic Force Microscopy. *Science* **1993**, *262* (5133), 547−550.
(186) Wallqvist, V.; Claesson, P. M.; Swerin, A.; Östlund, C.; Schoelkopf, J.; Gane, P. A. C. Influence of Surface Topography on Adhesive and Long-Range Capillary Forces between Hydrophobic Surfaces in Water. *Langmuir* **2009**, *25* (16), 9197−9207.
(187) Hampton, M. A.; Nguyen, A. V. Nanobubbles and the Nanobubble Bridging Capillary Force. *Adv. Colloid Interface Sci.* **2010**, *154* (1−2), 30−55.
(188) Hou, D.; Wang, Z.; Wang, K.; Wang, J.; Lin, S. Composite Membrane with Electrospun Multiscale-Textured Surface for Robust Oil-Fouling Resistance in Membrane Distillation. *J. Membr. Sci.* **2018**, *546*, 179−187.
(189) Wang, Z.; Hou, D.; Lin, S. Composite Membrane with Underwater-Oleophobic Surface for Anti-Oil-Fouling Membrane Distillation. *Environ. Sci. Technol.* **2016**, *50* (7), 3866−3874.
(190) Qiu, H.; Peng, Y.; Ge, L.; Villacorta Hernandez, B.; Zhu, Z. Pore Channel Surface Modification for Enhancing Anti-Fouling Membrane Distillation. *Appl. Surf. Sci.* **2018**, *443*, 217−226.

https://dx.doi.org/10.1021/acsestengg.0c00025
ACS EST Engg. 2021, 1, 117−140

(191) Vrouwenvelder, H. S.; van Paassen, J. A. M.; Folmer, H. C.; Hofman, J. A. M. H.; Nederlof, M. M.; van der Kooij, D. Biofouling of Membranes for Drinking Water Production. *Desalination* **1998**, *118* (1−3), 157−166.
(192) Gryta, M. The Assessment of Microorganism Growth in the Membrane Distillation System. *Desalination* **2002**, *142* (1), 79−88.
(193) Krivorot, M.; Kushmaro, A.; Oren, Y.; Gilron, J. Factors Affecting Biofilm Formation and Biofouling in Membrane Distillation of Seawater. *J. Membr. Sci.* **2011**, *376* (1−2), 15−24.
(194) Frock, A. D.; Kelly, R. M. Extreme Thermophiles: Moving beyond Single-Enzyme Biocatalysis. *Curr. Opin. Chem. Eng.* **2012**, *1* (4), 363−372.
(195) Bogler, A.; Lin, S.; Bar-Zeev, E. Biofouling of Membrane Distillation, Forward Osmosis and Pressure Retarded Osmosis: Principles, Impacts and Future Directions. *J. Membr. Sci.* **2017**, *542*, 378−398.
(196) Bar-Zeev, E.; Passow, U.; Romero-Vargas Castrillón, S.; Elimelech, M. Transparent Exopolymer Particles: From Aquatic Environments and Engineered Systems to Membrane Biofouling. *Environ. Sci. Technol.* **2015**, *49* (2), 691−707.
(197) Bar-Zeev, E.; Berman-Frank, I.; Girshevitz, O.; Berman, T. Revised Paradigm of Aquatic Biofilm Formation Facilitated by Microgel Transparent Exopolymer Particles. *Proc. Natl. Acad. Sci. U. S. A.* **2012**, *109* (23), 9119−9124.
(198) Schneider, R. P.; Chadwick, B. R.; Jankowski, J.; Acworth, I. Determination of Physicochemical Parameters of Solids Covered with Conditioning Films from Groundwaters Using Contact Angles. Comparative Analysis of Different Thermodynamic Approaches Utilizing a Range of Diagnostic Liquids. *Colloids Surf., A* **1997**, *126* (1), 1−23.
(199) Phattaranawik, J.; Fane, A. G.; Pasquier, A. C. S.; Bing, W.; Wong, F. S. Experimental Study and Design of a Submerged Membrane Distillation Bioreactor. *Chem. Eng. Technol.* **2009**, *32* (1), 38−44.
(200) De Kerchove, A. J.; Elimelech, M. Impact of Alginate Conditioning Film on Deposition Kinetics of Motile and Nonmotile Pseudomonas Aeruginosa Strains. *Appl. Environ. Microbiol.* **2007**, *73* (16), 5227−5234.
(201) Ferrando, D.; Toubiana, D.; Kandiyote, N. S.; Nguyen, T. H.; Nejidat, A.; Herzberg, M. Ambivalent Role of Calcium in the Viscoelastic Properties of Extracellular Polymeric Substances and the Consequent Fouling of Reverse Osmosis Membranes. *Desalination* **2018**, *429*, 12−19.
(202) Qiu, G.; Ting, Y. P. Short-Term Fouling Propensity and Flux Behavior in an Osmotic Membrane Bioreactor for Wastewater Treatment. *Desalination* **2014**, *332* (1), 91−99.
(203) Fang, Y.; Al-Assaf, S.; Phillips, G. O.; Nishinari, K.; Funami, T.; Williams, P. A.; Li, A. Multiple Steps and Critical Behaviors of the Binding of Calcium to Alginate. *J. Phys. Chem. B* **2007**, *111* (10), 2456−2462.
(204) Qin, W.; Zhang, J.; Xie, Z.; Ng, D.; Ye, Y.; Gray, S. R.; Xie, M. Synergistic Effect of Combined Colloidal and Organic Fouling in Membrane Distillation: Measurements and Mechanisms. *Environ. Sci. Water Res. Technol.* **2017**, *3* (1), 119−127.
(205) Shao, S.; Liang, H.; Qu, F.; Li, K.; Chang, H.; Yu, H.; Li, G. Combined Influence by Humic Acid (HA) and Powdered Activated Carbon (PAC) Particles on Ultrafiltration Membrane Fouling. *J. Membr. Sci.* **2016**, *500*, 99−105.
(206) Srisurichan, S.; Jiraratananon, R.; Fane, A. G. Humic Acid Fouling in the Membrane Distillation Process. *Desalination* **2005**, *174*, 63−72.
(207) Zhao, K.; Sun, J.; Hu, C.; Qu, J. Membrane Fouling Reduction through Electrochemically Regulating Flocs Aggregation in an Electro-Coagulation Membrane Reactor. *J. Environ. Sci.* **2019**, *83*, 144−151.
(208) Etchepare, R.; Oliveira, H.; Azevedo, A.; Rubio, J. Separation of Emulsified Crude Oil in Saline Water by Dissolved Air Flotation with Micro and Nanobubbles. *Sep. Purif. Technol.* **2017**, *186*, 326−332.
(209) Khuntia, S.; Majumder, S. K.; Ghosh, P. Microbubble-Aided Water and Wastewater Purification: A Review. *Rev. Chem. Eng.* **2012**, *28* (4−6), 191−221.
(210) Agarwal, A.; Ng, W. J.; Liu, Y. Principle and Applications of Microbubble and Nanobubble Technology for Water Treatment. *Chemosphere* **2011**, *84* (9), 1175−1180.
(211) Agarwal, A.; Xu, H.; Ng, W. J.; Liu, Y. Biofilm Detachment by Self-Collapsing Air Microbubbles: A Potential Chemical-Free Cleaning Technology for Membrane Biofouling. *J. Mater. Chem.* **2012**, *22* (5), 2203−2207.
(212) Qasim, M.; Darwish, N. N.; Mhiyo, S.; Darwish, N. A.; Hilal, N. The Use of Ultrasound to Mitigate Membrane Fouling in Desalination and Water Treatment. *Desalination* **2018**, *443*, 143−164.
(213) Hsu, S. T.; Cheng, K. T.; Chiou, J. S. Seawater Desalination by Direct Contact Membrane Distillation. *Desalination* **2002**, *143* (3), 279−287.
(214) Hou, D.; Lin, D.; Zhao, C.; Wang, J.; Fu, C. Control of Protein (BSA) Fouling by Ultrasonic Irradiation during Membrane Distillation Process. *Sep. Purif. Technol.* **2017**, *175*, 287−297.
(215) Zhu, J.; An, H.; Alheshibri, M.; Liu, L.; Terpstra, P. M. J.; Liu, G.; Craig, V. S. J. Cleaning with Bulk Nanobubbles. *Langmuir* **2016**, *32* (43), 11203−11211.
(216) Wu, Z. H.; Chen, H. B.; Dong, Y. M.; Mao, H. L.; Sun, J. L.; Chen, S. F.; Craig, V. S. J.; Hu, J. Cleaning Using Nanobubbles: Defouling by Electrochemical Generation of Bubbles. *J. Colloid Interface Sci.* **2008**, *328* (1), 10−14.
(217) Liu, G.; Wu, Z.; Craig, V. S. J. Cleaning of Protein-Coated Surfaces Using Nanobubbles: An Investigation Using a Quartz Crystal Microbalance. *J. Phys. Chem. C* **2008**, *112* (43), 16748−16753.
(218) Ebrahim, S. Cleaning and Regeneration of Membranes in Desalination and Wastewater Applications: State-of-the-Art. *Desalination* **1994**, *96* (1−3), 225−238.
(219) Huang, Y. X.; Wang, Z.; Jin, J.; Lin, S. Novel Janus Membrane for Membrane Distillation with Simultaneous Fouling and Wetting Resistance. *Environ. Sci. Technol.* **2017**, *51* (22), 13304−13310.
(220) Wang, Z.; Lin, S. The Impact of Low-Surface-Energy Functional Groups on Oil Fouling Resistance in Membrane Distillation. *J. Membr. Sci.* **2017**, *527*, 68−77.
(221) Wang, Z.; Jin, J.; Hou, D.; Lin, S. Tailoring Surface Charge and Wetting Property for Robust Oil-Fouling Mitigation in Membrane Distillation. *J. Membr. Sci.* **2016**, *516*, 113−122.
(222) Ulbricht, M. Advanced Functional Polymer Membranes. *Polymer* **2006**, *47* (7), 2217−2262.
(223) Boo, C.; Hong, S.; Elimelech, M. Relating Organic Fouling in Membrane Distillation to Intermolecular Adhesion Forces and Interfacial Surface Energies. *Environ. Sci. Technol.* **2018**, *52* (24), 14198−14207.
(224) Wang, Y. N.; Tang, C. Y. Protein Fouling of Nanofiltration, Reverse Osmosis, and Ultrafiltration Membranes-The Role of Hydrodynamic Conditions, Solution Chemistry, and Membrane Properties. *J. Membr. Sci.* **2011**, *376* (1−2), 275−282.
(225) Van Wagner, E. M.; Sagle, A. C.; Sharma, M. M.; La, Y. H.; Freeman, B. D. Surface Modification of Commercial Polyamide Desalination Membranes Using Poly(Ethylene Glycol) Diglycidyl Ether to Enhance Membrane Fouling Resistance. *J. Membr. Sci.* **2011**, *367* (1−2), 273−287.
(226) Choudhury, R. R.; Gohil, J. M.; Mohanty, S.; Nayak, S. K. Antifouling, Fouling Release and Antimicrobial Materials for Surface Modification of Reverse Osmosis and Nanofiltration Membranes. *J. Mater. Chem. A* **2018**, *6* (2), 313−333.
(227) Miller, D. J.; Dreyer, D. R.; Bielawski, C. W.; Paul, D. R.; Freeman, B. D. Surface Modification of Water Purification Membranes. *Angew. Chem., Int. Ed.* **2017**, *56* (17), 4662−4711.
(228) Liu, C.; Chen, L.; Zhu, L. Fouling Mechanism of Hydrophobic Polytetrafluoroethylene (PTFE) Membrane by Differently Charged Organics during Direct Contact Membrane Distillation (DCMD) Process: An Especial Interest in the Feed Properties. *J. Membr. Sci.* **2018**, *548*, 125−135.

https://dx.doi.org/10.1021/acsestengg.0c00025
ACS EST Engg. 2021, 1, 117−140

(229) Combe, C.; Molis, E.; Lucas, P.; Riley, R.; Clark, M. M. The Effect of CA Membrane Properties on Adsorptive Fouling by Humic Acid. *J. Membr. Sci.* **1999**, *154* (1), 73−87.
(230) Kochkodan, V.; Hilal, N. A Comprehensive Review on Surface Modified Polymer Membranes for Biofouling Mitigation. *Desalination* **2015**, *356*, 187−207.
(231) Li, F.; Meng, J.; Ye, J.; Yang, B.; Tian, Q.; Deng, C. Surface Modification of PES Ultrafiltration Membrane by Polydopamine Coating and Poly(Ethylene Glycol) Grafting: Morphology, Stability, and Anti-Fouling. *Desalination* **2014**, *344*, 422−430.
(232) Razmjou, A.; Arifin, E.; Dong, G.; Mansouri, J.; Chen, V. Superhydrophobic Modification of TiO2 Nanocomposite PVDF Membranes for Applications in Membrane Distillation. *J. Membr. Sci.* **2012**, *415−416*, 850−863.
(233) Hou, D.; Christie, K. S. S.; Wang, K.; Tang, M.; Wang, D.; Wang, J. Biomimetic Superhydrophobic Membrane for Membrane Distillation with Robust Wetting and Fouling Resistance. *J. Membr. Sci.* **2020**, *599*, 117708.
(234) Shan, H.; Liu, J.; Li, X.; Li, Y.; Tezel, F. H.; Li, B.; Wang, S. Nanocoated Amphiphobic Membrane for Flux Enhancement and Comprehensive Anti-Fouling Performance in Direct Contact Membrane Distillation. *J. Membr. Sci.* **2018**, *567*, 166−180.
(235) Zhu, Z.; Liu, Z.; Zhong, L.; Song, C.; Shi, W.; Cui, F.; Wang, W. Breathable and Asymmetrically Superwettable Janus Membrane with Robust Oil-Fouling Resistance for Durable Membrane Distillation. *J. Membr. Sci.* **2018**, *563*, 602−609.
(236) Chew, N. G. P.; Zhao, S.; Malde, C.; Wang, R. Superoleophobic Surface Modification for Robust Membrane Distillation Performance. *J. Membr. Sci.* **2017**, *541*, 162−173.
(237) Chew, N. G. P.; Zhang, Y.; Goh, K.; Ho, J. S.; Xu, R.; Wang, R. Hierarchically Structured Janus Membrane Surfaces for Enhanced Membrane Distillation Performance. *ACS Appl. Mater. Interfaces* **2019**, *11* (28), 25524−25534.
(238) Li, C.; Li, X.; Du, X.; Tong, T.; Cath, T. Y.; Lee, J. Antiwetting and Antifouling Janus Membrane for Desalination of Saline Oily Wastewater by Membrane Distillation. *ACS Appl. Mater. Interfaces* **2019**, *11* (20), 18456−18465.
(239) Chen, Y.; Lu, K. J.; Chung, T.-S. An Omniphobic Slippery Membrane with Simultaneous Anti-Wetting and Anti-Scaling Properties for Robust Membrane Distillation. *J. Membr. Sci.* **2020**, *595*, 117572.
(240) Lu, X.; Peng, Y.; Ge, L.; Lin, R.; Zhu, Z.; Liu, S. Amphiphobic PVDF Composite Membranes for Anti-Fouling Direct Contact Membrane Distillation. *J. Membr. Sci.* **2016**, *505*, 61−69.

https://dx.doi.org/10.1021/acsestengg.0c00025
ACS EST Engg. 2021, 1, 117−140